THE ROLE OF FGF10 IN THE DEVELOPMENT OF MOUSE SPINAL CORD

IRINA DJAČKOVA

THIS THESIS IS SUBMITTED FOR THE DEGREE OF MASTER OF SCIENCE BY RESEARCH

UNIVERSITY OF EAST ANGLIA

SCHOOL OF BIOLOGICAL SCIENCES

OCTOBER 2011

ABSTRACT

Fibroblast growth factor 10 (Fgf10) has been shown to play multiple developmental roles and be of high importance for the development of such organs as limbs, lungs and heart. However, nothing is known about its putative roles in the development of spinal cord.

To begin investigation of potential roles of Fgf10 in the spinal cord, its expression pattern was examined using tissue from *Fgf10-LacZ* reporter mice. Fgf10 expression was detected through the expression of β-gal, *LacZ* gene product, either enzymatically with X-gal or by immmunostaining. To check the identity of β-gal expressing cells, double-immunostaining was performed on sections of *Fgf10-LacZ* mouse embryos with antibodies against β-galactosidase and Olig2 (as motor neuron and oligodendrocyte progenitor marker), NeuN and TuJ1 (neuronal markers), and Islet 1 and Lhx3 (transcription factors). To investigate the roles of Fgf10, *Fgf10* knockout mice were used. Spinal cord sections of wild type and Fgf10 knockout embryos were immunostained with antibodies against NeuN, Lhx3, Olig2 (as oligodendrocyte marker), Islet1 and TuJ1, and expression patterns were then compared in the sections of the same level.

Fgf10 was detected in the ventral region of the developing mouse spinal cord from E8.5 to E14.5 and timing of Fgf10 expression correlated with neurogenesis. Fgf10 was shown to be expressed in neurons from the early stage of their differentiation until they become mature motor neurons. Loss of Fgf10 did not seem to affect motor neuron generation, differentiation into particular neuronal subtypes, or their final positioning. However, in Fgf10 knockouts, medial motor column (MMC) appeared to be more dispersed and MMC axonal terminals seemed to be disordered.

These results suggest that Fgf10 is involved in the formation and maturation of motor neurons, possibly in synapse formation between motor neurons and their target muscles.

CONTENTS

ACKNOWLEDGEMENTS

Firstly, I would like to thank Dr. Mohammad Hajihosseini for his continual guidance, encouragement and inspiration, as well as for constructive criticism at all stages of my research, Dr. Jelena Gavrilovic for her support, help and advice on my project and Dr. Paul Thomas for his invaluable help with microscopy and related software.

In addition, I would like to thank Andrew Moore, whose dissertation project was a starting point for my research. Thanks to all members of M. K. Hajihosseini laboratory: Dr. Timothy Goodman, Niels Haan, Christina Stratford and Alaleh Najdi-Samiei, for their great help, support and useful discussions. Thanks, also, to all my friends and colleagues in the BMRC for their support.

Finally, I would like to thank my parents Alla and Andrey Djačkovi for their continuous support and patience.

1. INTRODUCTION

Development of the nervous system is a highly organized and complex process. Thousands of neuronal connections build an extremely structured network that makes up the functioning nervous system. The development of the vertebrate spinal cord, part of the central nervous system, has been well studied (Briscoe and Novitch, 2008). Within the spinal cord, specific neuronal subtypes are generated from neural progenitor cells in response to different types and concentrations of signals produced from within the neural tube and surrounding tissues. These signals regulate the expression of transcription factors, which specify the fate of neural progenitors as they differentiate into neurons. In the ventral region of the spinal cord there are at least 5 neuronal subtypes: four subtypes of ventral interneurons and one set of motor neurons (MN) (Dessaud et al., 2008). Motor neurons project their axons outside the CNS and innervate muscles (Eisen, 1999). They can be divided into upper and lower motor neurons, with their cell bodies located in the brain and in the spinal cord, respectively. Motor neurons are severely affected in motor neuron diseases (MND) (Corcia et al., 2008).

MND is a group of neurodegenerative disorders that comprise three main types, which affect different groups of motor neurons. Amyotrophic lateral sclerosis (ALS), the most common type of MND, affects both upper and lower motor neurons and results in muscle wasting, speech and swallowing problems (Carlesi et al., 2011). Progressive muscular atrophy (PMA), a less common type of MND, affects lower motor neurons and consequences are less severe than in patients with ALS - weakness and atrophy of the body muscles. Primary lateral sclerosis, a very rare form of MND, affects upper motor neurons and results in muscle weakness and spasticity, but not atrophy (Rowland, 2010). MND is sporadic in 90–95% of cases and familial in approximately 5–10%. While studying familial MND cases, mutations in genes that code for superoxide dismutase 1 (SOD1), transactive response DNA-binding protein 43 (TDP-43) and fused in sarcoma/translocated in liposarcoma (FUS/TLS), have been identified and linked to MND onset. However, in 90% of the cases, the cause of the disease is still unknown. Currently available treatments can only slow down the progression of the disease, but there is no cure, as no precise mechanisms that underlie neurodegeneration have been identified (Shaw, 2005; Traub et al., 2011).

Degeneration and death of motor neurons in MND diseases leads to outcomes that are severe and often lethal, most people with MND die within five years of the onset of symptoms (Kanning et al., 2010). In the United Kingdom there are approximately 5000 individuals suffering from MND, of which more than a thousand die each year (Shaw, 2005).

In the light of this, it is of great importance to study molecular mechanisms of motor neuron development. A better knowledge of normal neural development is likely to help uncover the mechanisms of neurodegenerative diseases and contribute to the development of treatments for the repair of damaged nervous system. Also, knowledge about normal motor neuron development can be used to direct differentiation of stem cells *in vitro* to specific neuronal subtypes, which in future could be used to replace damaged nervous tissue.

1.1. Structure of the vertebrate nervous system

The vertebrate nervous system can be divided into the peripheral and the central nervous systems. The central nervous system (CNS) consists of the brain and the spinal cord. The peripheral nervous system branches outside from the CNS and is comprised of nerves and clusters of neurons called ganglia.

The CNS is made up of two principle cell types: neurons and glial cells. Neurons, generated by radial glial cells, are electrically excitable cells that process and transmit information by electrical and chemical signalling. The three basic classes of neurons are sensory neurons, motor neurons and interneurons. Sensory neurons process and relay sensory input, motor neurons project their axons outside the CNS and synapse muscle fibres and glands, and interneurons conduct and interpret impulses from one neuron to another (Slack 2006).

Glial cells, which include astrocytes, oligodendrocytes and microglia, provide support and protection for neurons. In contrast to other glial cells that are derived from neural plate, microglia are derived from bone marrow (Chan et al., 2007; Kettenmann et al., 2011). Oligodendrocytes form the myelin sheath around axons and support the long-term integrity of those axons (Nave, 2010). Astrocytes play a role in glutamate release and removal, which is important for neurotransmission, provide nutrients to neurons and remove debris of dead neurons (Lee and Pow, 2010). Microglia act as phagocytes and represent immune cells of the CNS (Kettenmann et al., 2011).

1.2. Structure of the developing mouse spinal cord

The developing mouse spinal cord consists of an inner neuroepithelial layer and a central area of grey matter (Leclerc et al., 2011). An outer layer of white matter appears postnatally, when mature oligodendrocytes create myelin sheath around axons (Doretto et al., 2011). The neuroepithelial layer, also called the ventricular zone, lines the lumen of the neural tube and functions as a repository of neural stem cells and later gives rise to ependyma (Leclerc et al., 2011). The grey matter is mainly comprised of cell bodies of postmitotic neurons. In the

grey matter, motor neurons are located ventrally, whereas interneurons and commissural neurons, which connect one side of the spinal cord with the other, are primarily found dorsally; the sensory neurons are found in the dorsal root ganglia. In addition to the neuronal cells, there are specialized cells that form the floor plate in the ventral midline and roof plate in the dorsal midline (Fig. 1.1). (Wolpert et al., 2007; Slack, 2006).

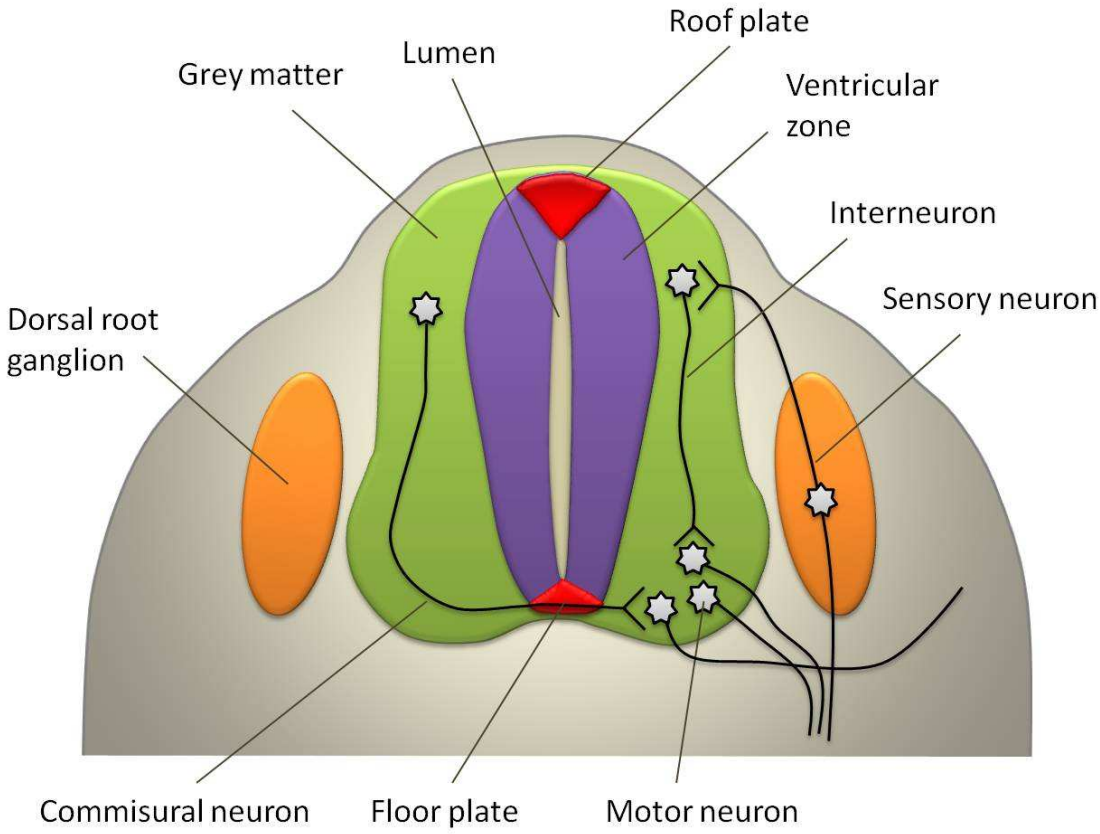

Fig. 1.1. Main structures of the developing spinal cord.

1.3. Development of the mouse spinal cord

Molecular mechanisms that underlie spinal cord development have been well characterized (Briscoe and Novitch, 2008). Within the spinal cord, ventricular zone cells are organized into distinct progenitor domains in response to signals produced from the neural tube and surrounding tissues. These signals regulate expression of transcription factors, which unique combination specifies each progenitor domain that later produces specific neuronal subtypes (Dessaud et al., 2008). When neurons become post-mitotic, they migrate outwards building concentric layers of cells in the spinal cord (Wolpert et al., 2007).

Spinal cord development, for convenience, is usually divided into stages; it begins with neural induction and is followed by rostrocaudal and dorsoventral patterning and a variety of secondary patterning events (Bronner-Fraser and Fraser, 1997).

1.3.1. Neural induction

The future CNS appears as the neural plate at embryonic day (E) 7 in the mouse embryo as a result of neural induction (Watson et al., 2008). Neural induction is the formation of neuroepithelium from the ectoderm in the dorsal region of the embryo in response to signals from the underlying mesoderm. The neural ectoderm thickens to form the neural plate, which in the following days folds and forms the neural tube (Sanes et al., 2006). The neural tube closes by E9.5-10 in the mouse embryo (Watson et al., 2008).

1.3.2. Rostrocaudal patterning

Rostrocaudal body axis, including the spinal cord, is patterned by *Hox* genes, members of the large family of homeobox genes. In vertebrates, *Hox* genes form four separate clusters. A unique feature of *Hox* gene expression is that the genes in the clusters are expressed in the same spatial and temporal order that they are positioned on the chromosome. The genes lying closer to 3` end in the cluster are expressed earlier and more rostrally in the rostrocaudal axis than genes lying more 5`(Kmita and Duboule, 2003).

Hox genes start to be expressed in the mouse embryo at the beginning of gastrulation and defined patterns of gene expression are seen in the mesoderm after somite formation and in the neural tube after its closure. *Hox* genes encode transcription factors, which specify rostrocaudal body axis into distinct regions and determine subsequent development of a region, for example, each somite can be specified by an exclusive pattern of *Hox* gene expression (Wolpert et al., 2007). In addition, *Hox* gene expression is critical for motor neuron differentiation. Members of *Hox* gene family specify identity of motor neuron columns, identity of motor neuron pools and define the pattern of target-muscle connectivity (Dasen et al., 2005).

The expression of *Hox* genes within the CNS is under control of several signalling molecules including fibroblast growth factors (Fgfs), retinoids, Wnts, and members of the transforming growth factor beta (TGF-β) superfamily. Graded Fgf signalling is involved in the induction of *Hox* gene expression at brachial, thoracic and lumbar levels of the spinal cord (Dasen et al., 2003). At more rostral levels, *Hox* genes are regulated by graded retinoic acid (RA) signalling, provided by paraxial mesoderm and somites, while at more caudal levels *Hox* genes are controlled by graded TGF-β family member, Gdf11, which acts in concert with high levels of Fgf signalling (Fig. 1.2) (Dasen and Jessell, 2009).

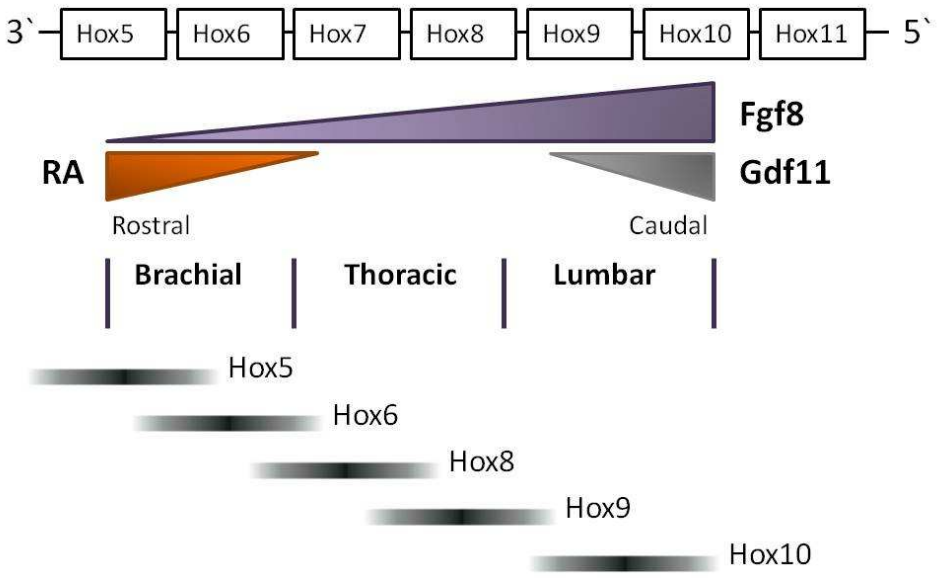

Fig. 1.2. Rostrocaudal patterning of the neural tube. Hox genes positioned closer to 3` end of the chromosome are expressed more rostrally, while genes lying more 5` are expressed more caudally. Graded Fgf signalling induces the expression of Hox genes along the rostrocaudal axis in the neural tube. Graded retinoic acid (RA) signalling regulates Hox gene expression rostrally, while at more caudal levels Hox genes are controlled by graded Gdf11 (Adapted from Dasen and Jessell, 2009).

1.3.3. Dorsoventral patterning

The initial dorsoventral patterning is set up by several extracellular signalling molecules; these include Fgf8, Retinoic Acid, Wnts, Bone morphogenetic proteins (BMPs) and Sonic Hedgehog (Shh) (Fig. 1.3). It is commonly acknowledged that BMPs, Wnts and Shh are the main players in patterning dorsoventral axis of the spinal cord (Wilson and Maden, 2005). BMPs, expressed by the overlying dorsal ectoderm and roof plate cells, specify neuronal fate in the dorsal neural tube and, also, inhibit the specification of the ventral neural tube cells. In addition to BMPs, Wnt proteins emanating from the dorsal midline have also been found to play role in neural progenitor behaviour and neuronal identity (Muroyama et al., 2002; Ulloa and Marti, 2010). Sonic Hedgehog, expressed by the notochord and the floor plate, specifies the pattern of ventral neurogenesis by providing specific identity and positional information to ventral neural progenitor cells (Ericson et al., 1996).

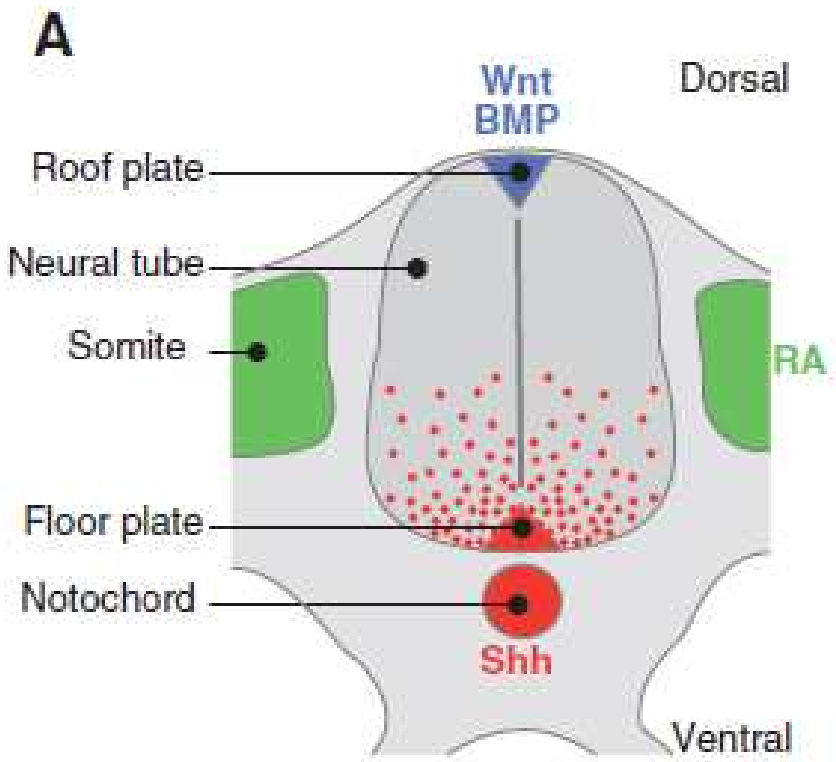

Fig. 1.3. Dorsoventral patterning of the neural tube. The key molecules that pattern dorsoventral axis of the neural tube include Sonic Hedgehog (Shh, red), secreted by the notochord and floor plate; retinoic acid (RA, green), produced by the somites; BMP and Wnt family members (blue), generated by the roof plate (Adapted from Dessaud et al., 2008).

Shh acts in a graded manner: neural progenitors located in more ventral regions of the neural tube are exposed to higher Shh concentration, than progenitors located more dorsally. A certain concentration of the Shh molecule is needed to generate each progenitor domain, which later will differentiate into distinct neuronal subtype. As a result, progenitor domains are generated and arranged in a precise spatial order along the dorsoventral axis (Dessaud et al., 2008). In the ventral spinal cord there are at least five progenitor domains: four domains of ventral interneuron progenitors (p0 – p3) and one domain of motor neuron and oligodendrocyte (MN/OL) progenitors (Fig. 1.4). A common progenitor for MN and oligodendrocytes produces motor neurons first and later in development, at E12.5-13, switches to production of oligodendrocyte precursors (Li et al., 2011).

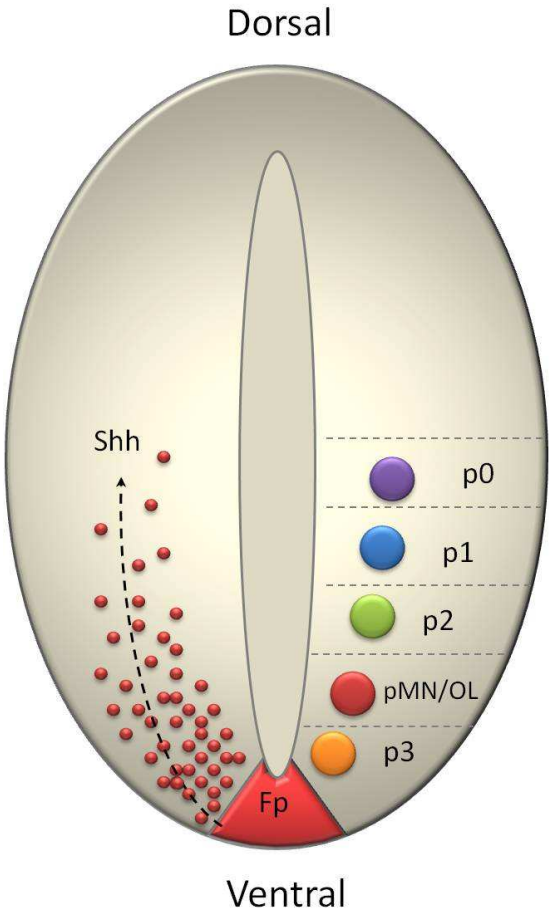

Fig. 1.4. Generation of distinct neuronal progenitor domains in the ventral spinal cord in response to graded Sonic Hedgehog signalling. Graded Shh signalling arranges neural progenitors into precise domains (p0-p3, pMN/pOL) along the dorsoventral axis of the spinal cord. Neural progenitors located more ventrally are exposed to higher concentration of Shh, than progenitors located more dorsally. Shh – Sonic Hedgehog; Fp-Floor plate; p0 – p3 – Progenitor domains of ventral interneurons; pMN/pOL – motor neuron and oligodendrocyte progenitor domain.

Shh signalling organizes neural progenitors into spatially distinct domains along the dorsoventral axis of the neural tube by regulating expression of transcription factors. Transcription factors expressed in neural progenitors can be divided into two groups, termed class I and II proteins, according to the effect of their regulation by Sonic Hedgehog signalling. Shh signalling represses the expression of class I proteins (Pax7, Irx3, Dbx1, Dbx2, and Pax6) and induces the expression of class II proteins (Dbx1, Dbx2, Nkx6.1, Olig2, Nkx2.2 and Foxa2) (Briscoe et al., 2000). Once expressed, class I and II proteins exhibit cross-repressive interactions, which help to define distinct progenitor domains. RA from the paraxial mesoderm and Fgf signalling also influence the pattern of transcription factors in progenitor cells. RA signalling induces the expression of class I proteins, whereas, Fgf signalling stops dorsoventral patterning by blocking both class I and II protein expression (Fig 1.5) (Briscoe and Novitch, 2008).

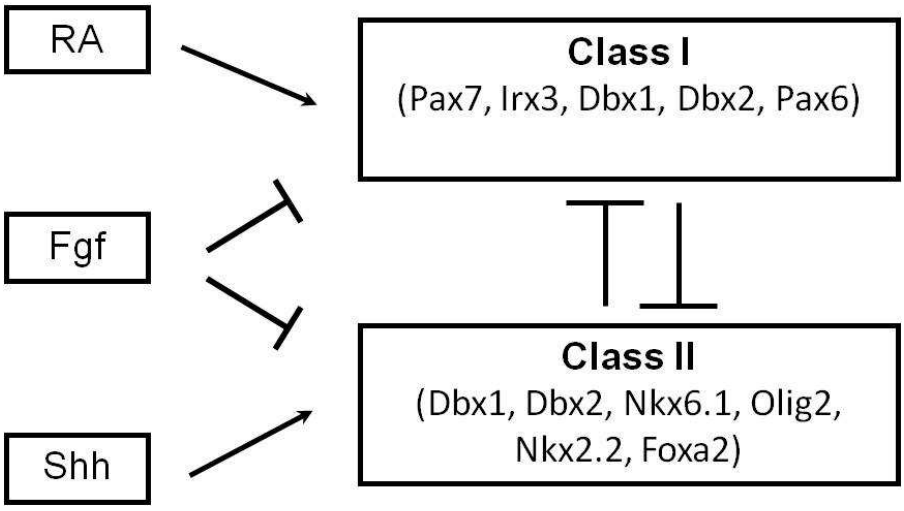

Fig. 1.5. Fgf, RA and Shh interaction with class I and II proteins. Fgf signalling suppresses expression of class I (Pax7, Irx3, Dbx1, Dbx2, and Pax6) and class II Dbx1, Dbx2, Nkx6.1, Olig2, Nkx2.2 and Foxa2) proteins. RA induces expression of class I proteins, whereas Shh signalling promotes expression of class II proteins. Once expressed, reciprocal pairs of class I and II proteins show cross-repressive interactions to generate discrete progenitor domains (Adapted from Briscoe and Novitch, 2008).

Transcription factors produce a unique transcriptional code for each progenitor subtype, e.g. motor neuron progenitors are identified by Nkx6.1, Nkx 6.2, Pax6 and Olig2 expression (Fig. 1.6). Distinct neuronal subtypes are generated in a precise spatial order from progenitor domains at E9-9.5 (Jessell, 2000).

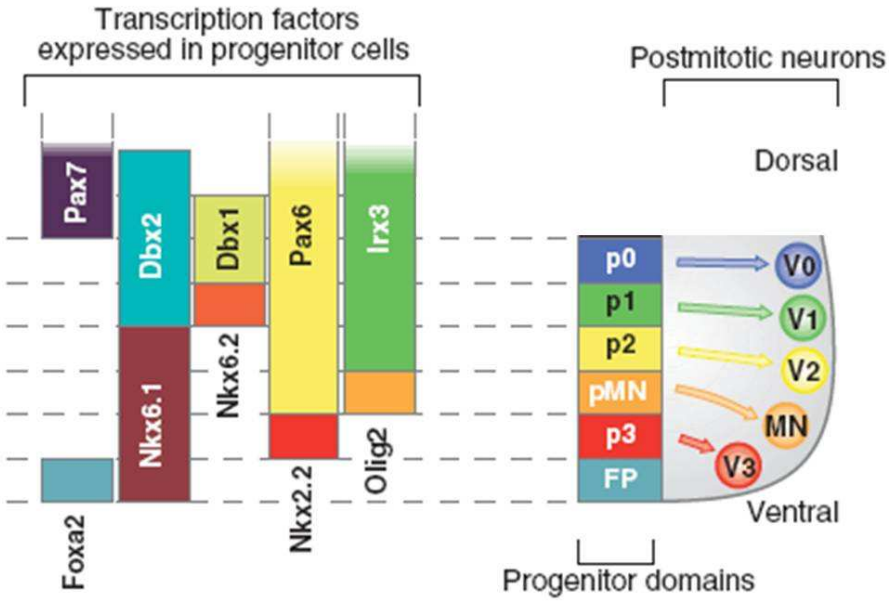

Fig. 1.6. A combinatorial expression of transcription factors in the ventral region of the spinal cord defines progenitor domains, which later generate distinct neuronal subtypes. Each progenitor domain is identified by its unique transcription factor code, which determines what neuronal subtype will be generated from a certain progenitor domain, e.g. motor neuron progenitors are identified by Nkx6.1, Nkx 6.2, Pax6 and Olig2 expression. Progenitor domains p0 - p3 generate different ventral interneuron subtypes (V0-V3), while motor neuron progenitors (pMN) produce motor neurons (MN). FP - floor plate (Adapted from Dessaud et al., 2008).

1.3.4. Motor neuron development in the mouse spinal cord

Motor neurons are easily identifiable, because they project axons out of the CNS and their activity can be recorded through their output – muscle contraction. Therefore, this class of neurons has been very well studied and is well characterized (Price and Briscoe, 2004).

Motor neuron development can be divided into four stages: first, specification and birth of motor neurons; second, migration of immature neurons to their final position in the spinal cord according to their motor column identity and projection of their axons towards their target regions; third, motor pool formation and establishment of synaptic connections and fourth, refinement of synaptic connections through the elimination of axon branches and cell death (Jessell, 2000, Wolpert et al., 2007).

The first stage of motor neuron development begins during dorsoventral patterning of the spinal cord. MN progenitor cells, one of the first progenitors to differentiate, are generated in a specific domain of ventricular zone in the ventral region of the spinal cord as described earlier. Ventral progenitors become specified into motor neuron and oligodendrocyte progenitors (MN/OL progenitors), when Olig2 expression is induced in response to continued

RA and Shh signaling (Novitch et al., 2003). Olig2 plays an important role in MN and oligodendrocyte (OL) generation and differentiation and has been shown to regulate fate switch in MN/OL progenitors by reversible phosphorylation on Serine 147. When Olig2 is phosphorylated, MN/OL progenitors generate MN, but Olig2 dephosphorylation triggers production of OL precursors (OLP) (Li et al., 2011). Motor neurons share the same population of progenitor cells with oligodendrocytes up to the point when Notch signalling is activated (Park and Appel, 2003). Notch signalling prevents expression of Ngn2 and maintains MN/OL progenitor cells in undifferentiated state until additional signals at E12.5-13, such as Olig2 dephosphorylation, promote MN/OL progenitors differentiation into OLP. Oligodendrocyte precursors subsequently migrate throughout the spinal cord before becoming myelinating oligodendrocytes (Cai et al., 2005; Park and Appel, 2003).

In the absence of Notch signaling, phosphorylated Olig2 promotes expression of Ngn2 and proneural protein NeuroM that cause MN/OL progenitors to become committed MN progenitors and begin to exit the cell cycle. Subsequent downregulation of Olig2 expression promotes differentiation of motor neurons (Fig. 1.7) (Briscoe and Novitch, 2008).

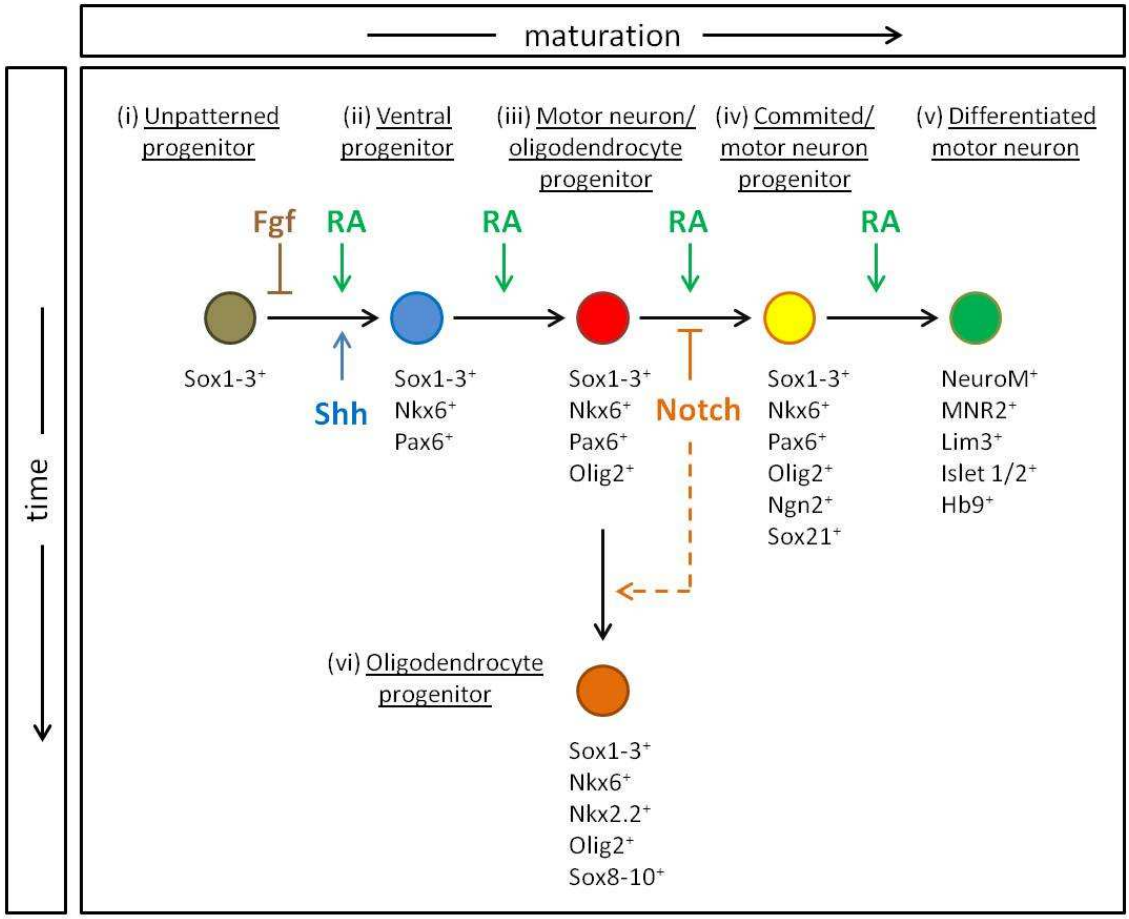

Fig 1.7. Changes in gene expression in progenitor cells during motor neuron development. (i) Neural progenitors expressing Sox1–3 are kept in an undifferentiated state as a result of Fgf signalling. (ii) Shh and RA signalling ventralizes neural progenitors by inducing expression of Nkx6 and Pax6 transcription factors. (iii) As a result of continued exposure to Shh and RA, Olig2 expression is induced in neural progenitors, which now can become both motor neurons and oligodendrocytes. (iv) In the presence of Notch signalling, progenitor cells express Ngn2 and Sox21, become committed motor neuron progenitors and begin to exit the cell cycle. (v) Ongoing RA acid signalling and downregulation of Olig2 expression promotes further differentiation of motor neurons. (vi) Activation of Notch signalling prevents the expression of Ngn2 in motor neuron/ oligodendrocyte progenitors and maintains these cells in an undifferentiated state until additional signals promote differentiation into oligodendrocytes (Adapted from Briscoe and Novitch, 2008).

The second stage of motor neuron development begins after motor neurons are born. Spinal motor neurons are one of the first neurons to be born. The time when neurons are born is defined by the last mitotic division of its progenitor cell (Watson et al., 2008). In mice, motor neurons are born between E 9.5 and E13. First motor neurons are born in the brachial region folloed by more caudal regions - thoracic and lumbar regions (Nornes and Carry, 1978).

MN migrate out of the ventricular zone to settle in an appropriate position, depending on to which motor neuron subtype they belong to. MN are specified into subtypes and arranged into discrete motor columns depending on the muscles they innervate (Fig 1.8). In mice, MN

extend their axons into the periphery as early as E10. The median motor column (MMC) innervates axial muscles and is present at all levels of the spinal cord. The preganglionic column (PGC) innervates sympathetic ganglia and can be found only at thoracic levels, as well as the hypaxial motor column (HMC), that innervates body wall muscles. The lateral motor column (LMC) innervates limb muscles and, therefore, is generated only at limb levels of the spinal cord. The LMC can be divided further into a medial division (LMCm), that project axons to ventrally derived muscles and a lateral division (LMCl), that project axons to dorsally derived muscles (Dasen and Jessell, 2009; Kania et al., 2000).

Motor neurons are specified into subtypes by rostrocaudal patterning. Hox gene expression is critical for motor neuron columnar identity, motor pool identity and initial steps of axonogenesis. Expression of Hox genes defines the position in which distinct motor columns are generated. For example, Hox6 expression is restricted to brachial level, where LMC is generated, while Hox9 to thoracic level, where PGC and HMC are generated (Dasen and Jessell, 2009).

Hox genes function in a combinatorial manner with LIM homeodomain transcription factors: Islet 1, Islet 2, Lhx1 and Lhx3 to control motor neuron subtype identity. There are two layers of gene regulation to control motor axon projections. One of them is static and specifies MN subtypes into columns and pools, while the other layer changes actively and regulates motor axon pathfinding (Bonanomi and Pfaff, 2010).

Specific combinations of the LIM homeodomain transcription factors, which are static, identify motor column subtype: Islet 1, Islet 2 and Lhx3 are molecular markers of the MMC column; Islet 1 and Islet 2 define the HMC column; the combination of Islet 2 and Lhx1 identify the LMCl; Islet 1 and Islet 2 label the LMCm; and Islet 1 expression defines the PGC column (Fig. 1.8) (Dasen et al., 2003; Tsuchida et al., 1994).

Dynamic regulation of LIM homeodomain transcription factor expression guides the projection of motor neuron axons to specific muscles. For example, in MMC neurons, Lhx3 controls the expression of fibroblast growth factor receptor 1 (FgfR1), which makes them sensitive to dermomyotome-derived FGFs that act as strong chemoattractants for MMC axons (Shirasaki et al., 2006). In LMCl neurons, Lim1 has been linked to the control of EphA4 receptor, and in LMCm neurons Isl1 has been linked to EphB1receptor (Kania and Jessell, 2003; Luria et al., 2008). Also, Lhx3 expression has been shown to be necessary for MN axons to exit spinal cord ventrally. Initially, when MN are born, Lhx3 is expressed in all of them for a short period of time, and then is rapidly downregulated in all except the MMC neurons (Sharma et al., 1998). Shortly after motor axons exit the neural tube they select their innervation targets (Bonanomi and Pfaff, 2010).

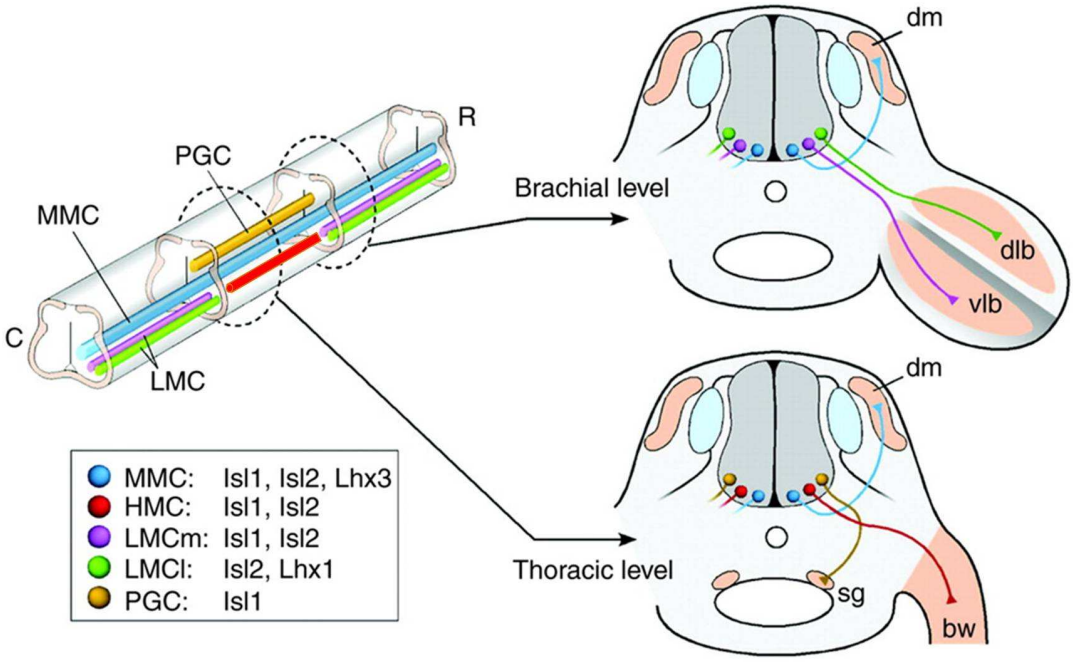

Fig. 1.8. Motor neuron columnar organization in the spinal cord. Motor neurons are segregated into longitudinal motor columns along the rostrocaudal axis of the spinal cord according to their innervation targets. The medial motor column (MMC, blue) neurons are generated at all rostrocaudal levels of the spinal cord and project axons to the axial muscles (dermomytome, dm). The lateral motor column (LMC) spanning brachial and lumbar levels of the spinal cord is further divided into lateral (LMCl, green) and medial (LMCm, purple) divisions, which project axons to muscles of dorsal (dlb) and ventral limb bud (vlb) respectively. Preganglionic motor column (PGC, orange) neurons, which innervate sympathetic ganglia (sg), and hypaxial motor column (HMC, red) neurons, which innervate body wall muscles (bw), are located at thoracic levels. A unique combination of LIM homeodomain transcription factors identifies motor column subtype: Islet 1, Islet 2 and Lhx3 characterize MMC column; Islet 1 and Islet 2 are specific for the HMC column; the combination of Islet 2 and Lhx1 identifies the LMCl; Islet 1 and Islet 2 label the LMCm and Islet 1 expression defines the PGC column. C - caudal. R – rostral (Adapted from Bonanomi and Pfaff, 2010).

The third stage starts at about E11.5-12 when LMC axons begin to sort into medial and lateral divisions and into motor pools. A motor pool is a group of motor neurons that innervate the same muscle. The existence of a great variety of muscle groups in the limbs demands an equivalent diversity of motor pools (Dasen et al., 2005). Motor pool identity is also controlled by Hox genes (Dasen and Jessell, 2009).

Once MN axons have arrived at their target, the formation of synapses begins. Before an axon terminal has approached, acetylcholine receptors become concentrated in the central region of the muscle fibre. When the motor axon arrives, it secretes Agrin into the basal lamina, which induces clustering of acetylcholine receptors and specialization of muscle cell surface. Signals from the muscle in turn promote differentiation of the pre-synaptic zone on the axon terminal and align it with the post-synaptic area. Process of MN axon projection and synapse

formation is very accurate, although, some pathfinding errors take place and they are eliminated by editing during the fourth stage (Colon-Ramos, 2009).

The fourth stage begins at about E12, shortly after MN axons reach their targets and includes refinement of synaptic connections through the elimination of axon branches and cell death (Yamamoto and Henderson, 1999). Once a motor neuron axon has established a contact with a muscle cell, it can activate the muscle, and this is followed by the death of the other MN that were navigating to the same muscle cell. Nevertheless, some muscle fibres become innervated by several axon terminals and then most connections are eliminated by programmed cell death, until each muscle fibre is innervated by one axon (Wolpert et al., 2007).

1.4. Fibroblast growth factor signalling system

14.1. Fibroblast growth factors

The mammalian Fibroblast growth factor (Fgf) signalling system consists of Fgfs that act as extracellular ligands that bind to and activate four receptor tyrosine kinases termed FgfR1, FgfR2, FgfR3 and FgfR4 (Eswarakumar et al., 2005). Fibroblast growth factors comprise a large family of signalling molecules that have been found both in invertebrates and vertebrates. The Fgf family consists of 22 members in mouse (Fgf 1-18, 20-23) and in human (FGF 1-14, 16-23) (Ornitz and Itoh, 2001).

The molecular weight of vertebrate Fgf`s varies from 17 to 34 kDa. Gene structure and amino-acid sequence of Fgfs are highly preserved between vertebrates and all the members of the family share a conserved 120- amino acid residue core with 16% to 65% amino acid similarity (Eswarakumar et al., 2005).

Vertebrate Fgfs can be classified into seven subfamilies by phylogenetic analysis: *Fgf1 (1,2), Fgf4 (4,5,6), Fgf7 (3,7,10,22), Fgf8 (8,17,18), Fgf9 (9,16,20), iFgfs (11,12,13,14),* and *hFgfs (15, 21, 23)* (Fig 1.9). Members of a subfamily share high sequence similarity, similar receptor-binding properties and some overlapping sites of expression. For example within Fgf7 subfamily, Fgf10 has 60% amino acid sequence identity with Fgf7 and Fgf3, and members of the Fgf8 subfamily (Fgf8, Fgf17, and Fgf18) have 70-80% amino acid sequence identity (Maruoka et al., 1998; Yamasaki et al., 1996).

Fgf family proteins are expressed in many tissues, but the patterns and timing of expression are different. Some Fgfs are expressed only in embryonic tissues (Fgf3, 4, 8, and 17), whereas others are expressed in embryonic and adult tissues. Patterns of Fgfs expression

suggest that they play vital roles in organism development and repair. During embryonic development Fgfs have diverse roles in regulating cell proliferation, migration and differentiation (Ornitz and Itoh, 2001). For example, Fgf10 has been shown to promote proliferation of epithelial progenitor cells during pancreatic organogenesis (Bhushan et al., 2001). Fgf2 and Fgf4 *in vitro* stimulate migration of myogenic cells in mouse embryonic limbs (Webb et al., 1997). Fgf18 is required for cell proliferation and differentiation during osteogenesis (Ohbayashi et al., 2002). In the adult, Fgfs act as homeostatic factors and play significant roles in cell differentiation, tissue repair and wound healing (Eswarakumar et al., 2005; Ornitz and Itoh, 2001). Fgf7 and Fgf10 have been shown to play an important role in skin wound healing (Komi-Kuramochi et al., 2005).

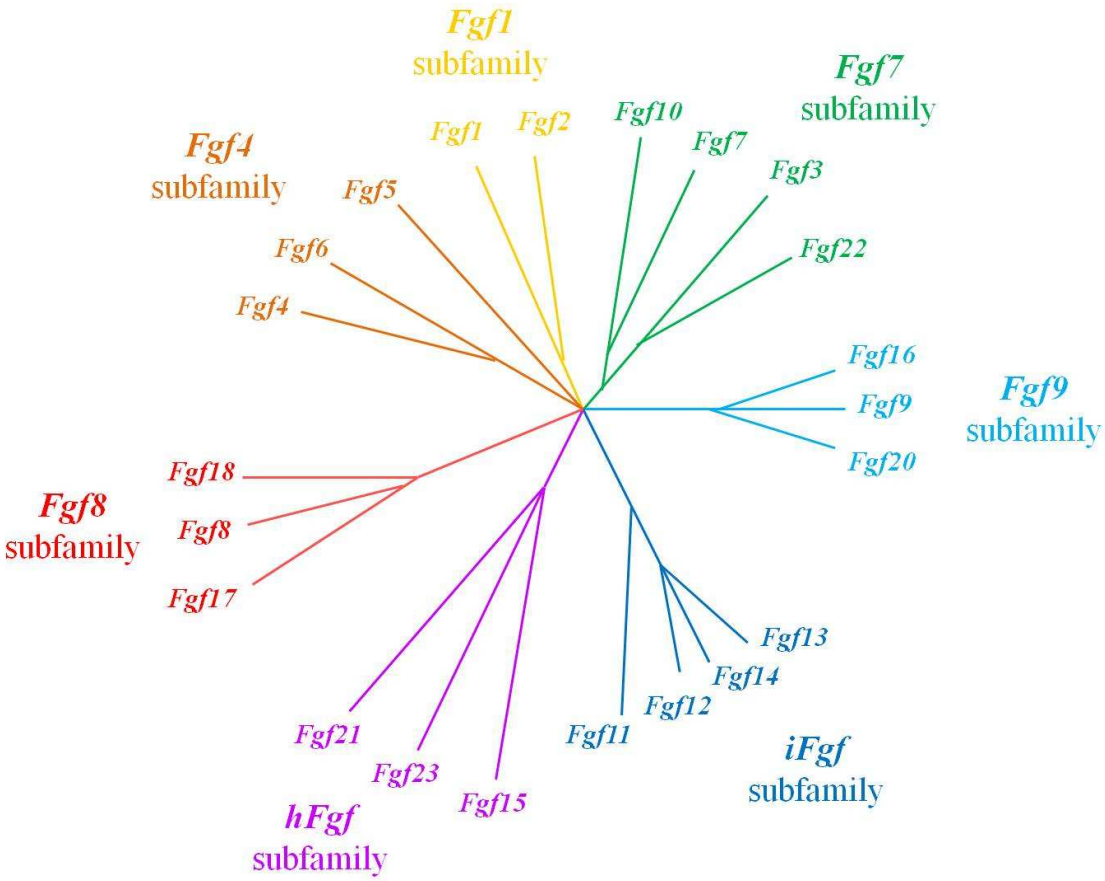

Fig. 1.9. Phylogenic tree of mouse *Fgf* gene family. Mouse *Fgf* gene family can be divided into seven subfamilies containing two to four members each. Branch lengths are proportional to the evolutionary distance between each gene (Adapted from Itoh and Ornitz, 2008).

1.4.2. Fibroblast growth factor receptors

In human and mice there are four *FgfR* genes, *FgfR1 – FgfR4*, that encode four FgfR tyrosine kinase receptors FgfR1-4. FgfRs are comprised of an extracelullar ligand binding domain that consists of three immunoglobulin-like (Ig-like) domains (I, II, III), a transmembrane domain and a cytoplasmic tyrosin kinase domain (Jaye et al., 1992).

A significant characteristic of the FgfR family is a variety of isoforms that are generated by alternative mRNA splicing of FgfR 1, 2 and 3, but not FgfR4 transcripts. Alternative splicing of exons 8 and 9 generates either IIIb or IIIc isoforms of FgfR: splicing of exons 7 and 8 generates FgfR-IIIb isoform, while combination of exons 7 and 9 generates the FgfR-IIIc isoform (Fig. 1.10) (Eswarakumar et al., 2005).

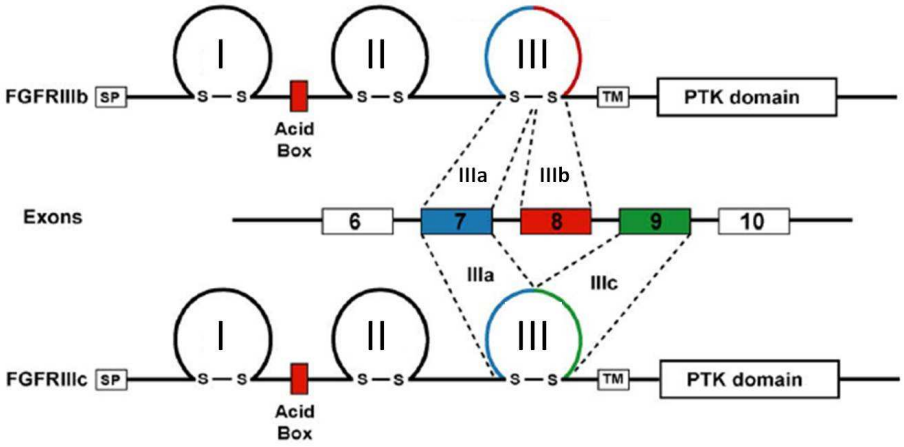

Fig. 1.10. Structure of FgfR isoforms generated by alternative splicing of FgfR transcripts. FgfR consists of three immunoglobulin-like (Ig-like) domains (I, II, III), a transmembrane domain (TM) and a protein tyrosin kinase domain (PTK). SP - signal peptide. The b and c isoforms of FgfR are produced in the result of alternative splicing of exons 8 and 9. Combination of exons 7 and 8 generates FgfR-IIIb isoform, while combination of exons 8 and 9 generates the FgfR-IIIc isoform. (Adapted from Eswarakumar et al., 2005).

Consequently, seven FgfR proteins (Fgfrs 1IIIb, 1IIIc, 2IIIb, 2IIIc, 3IIIb, 3IIIc, and 4) are generated from four *FgfR* genes. Difference between the isoforms is found in the third Ig-like domain and changes ligand-binding specificity. For example FgfR2-IIIb isoform binds Fgf7, Fgf10 and Fgf22, but not Fgf4 or Fgf6 that activate FgfR2-IIIc. The specificity of these isoforms towards various Fgf ligands is summarized in the table below (Table 1.1) (Eswarakumar et al., 2005).

Fgfr isoform	Ligand specifisity
FgfR1-IIIb	Fgf 1, -2, -3 and -10
FgfR1-IIIc	Fgf 1, -2, -4, -5 and -6
FgfR2-IIIb	Fgf 1, -3, -7, -10 and -22
FgfR2-IIIc	Fgf 1, -2, -4, -6, -9, -17
FgfR3-IIIb	Fgf 1 and -9
FgfR3-IIIc	Fgf 1, -2, -4, -8, -9, -17, -
FgfR4	Fgf 1, -2, -4, -6, -8, -9, -

Table 1.1. Ligand specificities of Fgfr isoforms

1.4.3. Fgf signalling through FgfRs

Fgf family contains 22 members, however, only 18 of them act through FgfRs. Members of iFgf subfamily (Fgf11-14) do not mediate their response by activating FgfRs and are called homologous factors (Itoh and Ornitz, 2008; Smallwood et al., 1996). iFgfs lack signal sequences and are considered to have an intracellular role (Itoh and Ornitz, 2008). Fgf1 and Fgf2, also, lack signal sequences and hence are not secreted, though, they can be found on the cell surface and extracellular matrix (Ornitz and Itoh, 2001).

Secreted Fgfs act as signal molecules that bind and activate FgfRs. FgfRs get activated when Fgf ligand, bound to heparan sulfate proteoglycans (HSPG), binds to the receptor causing its dimerization. HSPG act as a low-affinity receptor that does not transmit signal, but functions as an accessory molecule and has been shown to increase affinity and half-life of the Fgf-FgfR complex (Eswarakumar et al., 2005; Ornitz and Itoh, 2001). Also, Fgf interaction with HSPG stabilizes Fgfs to thermal denaturation and proteolysis (Ornitz and Itoh, 2001).

FgfRs mediate their signalling by recruiting specific proteins that bind to tyrosine auto-phosphorylation sites on the activated receptor and by using docking proteins that become tyrosine phosphorylated in response to Fgf-stimulation. Fgf-stimulation of docking proteins of the FRS2 family results in activation of the Ras/ mitogen - activated protein (MAP) kinase and phosphatidylinositol - 3 (PI-3) kinase signalling pathways (Eswarakumar et al., 2005; Kouhara et al., 1997)

1.5. Fgf signalling in the developing mouse spinal cord

1.5.1. Fgfs and FgfRs involved in the development of mouse spinal cord

Fgf signalling plays an important role in the development of the CNS. There have been multiple studies on Fgf expression during brain development, while Fgf contribution to spinal cord development still has to be described in more details (Ford-Perriss et al., 2001).

Three out of four FgfR receptors have been detected in the developing mouse spinal cord by Shirasaki in 2006, however, receptor isoforms have not been specified. FgfR1 expression localizes in the ventral horns of the spinal cord, while FgfR2 and FgfR3 are expressed in the ventricular zone (Shirasaki et al., 2006). Later, Fon Tacer showed in 2010 that FgfR-IIIc isoform is predominant in adult mouse CNS, including the spinal cord (Fon Tacer et al., 2010).

Fgfs are expressed in the spinal cord from the very beginning of its formation. Fgfs are required for the neural induction and generation of neural tissue (Wilson and Maden, 2005). A gradient of Fgf8, in particular, is necessary for the induction of Hox genes that are essential for patterning the rostrocaudal axis of the neural tube (Crossley and Martin, 1995).

A number of Fgfs have been shown to be expressed in the developing spinal cord e.g. Fgf1, Fgf2, Fgf9 and Fgf15 (Colvin et al., 1999; Ford-Perriss et al., 2001). Mouse Fgf2 mRNA has been shown to be expressed in the neural tube, including the ventricular zone, and within dorsal root ganglia (DRG) starting from E10, when neural crest precursors are proliferating within the DRG and consequently might play a role in the proliferation of neuronal precursors (Ford-Perriss et al., 2001; Murphy et al., 1994).

Fgf9 is strongly expressed in the developing motor neurons from E10 to E14 and its expression pattern suggests a role in the development and maintenance of motor neurons and a possible role in skeletal muscle innervation (Colvin et al., 1999; Garces et al., 2000).

Fgf15 is expressed in the dorsal region of the developing spinal cord from E8 to E14 and may play an important role in regulating cell division and patterning within the embryonic spinal cord (Ford-Perriss et al., 2001; McWhirter et al., 1997).

Recently, Fgf10 expression has been detected in the developing mouse spinal cord, which implicates it in mouse spinal cord development (unpublished data of M.K. Hajihosseini).

1.5.2. Fgf10 expression in the developing mouse spinal cord

Fgf10 encoding cDNA was originally isolated from rat embryos in 1996 (Yamasaki et al., 1996). It was soon followed by isolation of mouse Fgf10 cDNA, which encoded a secreted protein of 209 amino acids (Tagashira et al., 1997).

Fgf10 has been shown to play diverse roles in the development of many different tissues. So far, Fgf10 has been shown to play critical roles in limb and lung development and an important role in heart development (Abler et al., 2009; Kelly et al., 2001; Min et al., 1998; Vega-Hernandez et al., 2011; Zakany et al., 2007). Also, Fgf10 is essential for the development of pancreas, white adipose tissue, mammary glands, eyelids, intestine, liver and brain (Berg et al., 2007; Bhushan et al., 2001; Konishi et al., 2006; Mailleux et al., 2002; Nyeng et al., 2011; Sahara and O'Leary, 2009; Tao et al., 2005). At the meantime, studies to determine Fgf10 role in adult animals are limited, because *Fgf10* knockout mice die at birth (Min et al., 1998).

Fgf10 expression has, also, been detected in the spinal cord of juvenile and adult mice, aged 4 and 56 days, respectively (Allen Institute for Brain Science database) (Fig. 1.11). Despite the fact that *Fgf10* expression has been shown in the mouse spinal cord, at the moment, there are no publications related to possible Fgf10 roles in that region.

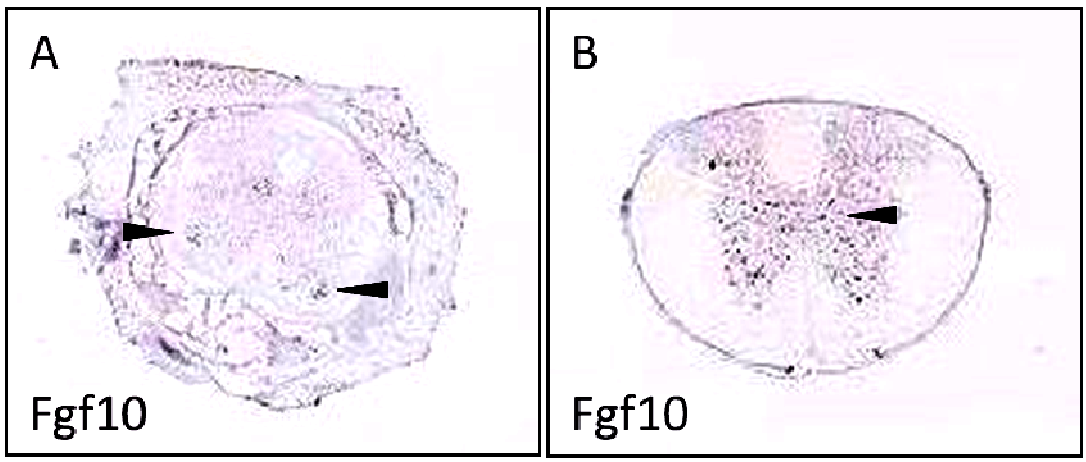

Fig 1.11. *In situ* hybridisation of Fgf10 in 4 days (A) and 56 days (B) old mouse spinal cord. (A) Transverse section of the spinal cord at thoracic level of 4 days old mouse; Fgf10 is expressed in the ventral horns of the spinal cord. (B) Transverse section of the spinal cord at thoracic level of 56 days old mouse; Fgf10 expressing cells are scattered across the spinal cord.

Recently, Fgf10 expression has been detected by *in situ* hybridisation in the spinal cord of E12.5 mouse embryo and it is the first evidence of Fgf10 expression in the developing mouse

spinal cord (unpublished data of M. K. Hajihosseini). At E12.5, Fgf10 is mainly localized in the ventral horns of the spinal cord, in the area where motor neurons normally reside (Fig. 1.12).

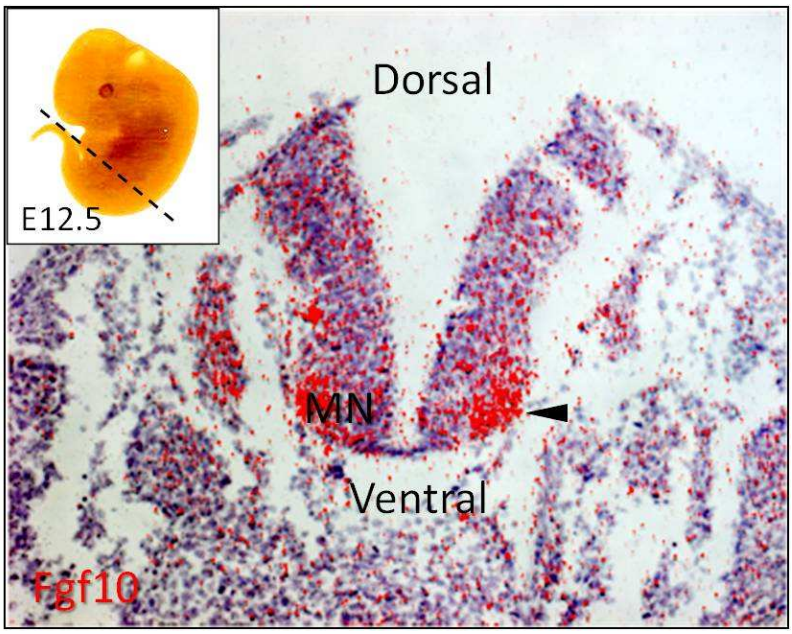

Fig. 1.12. ***In situ*** **hybridisation of Fgf10 in the E12.5 developing mouse spinal cord.** Please note that the section has been torn dorsally. Fgf10 expression is shown in red and is mainly localized in the ventral horns of the spinal cord (unpublished data of M.K. Hajihosseini).

1.6. Aims

Molecular pathways of spinal motor neuron development are among the most characterized ones. However our knowledge about relevant pathways of MN organization and differentiation is still incomplete. Recently, studies have shown that a member of the fibroblast growth factor family- *Fibroblast Growth Factor 10* (*Fgf10*) is expressed in the ventral part of the developing mouse spinal cord, in the region where motor neuron bodies usually are located (unpublished results of M. K. Hajihosseini).

During embryonic development, *Fgf10* is widely expressed in various tissues of the mouse organism, and is known to play a key role in the organogenesis of various organs, including lungs, pancreas, mammary glands, limbs and brain (Bellusci et al., 1997; Bhushan et al., 2001; Mailleux et al., 2002; Min et al., 1998; Sahara and O'Leary, 2009). Until now, *Fgf10* expression in the developing spinal cord has not been reported, and nothing is known about its possible function in that region.

In this report I examine the *Fgf10* expression pattern and investigate its role in the developing mouse spinal cord. Preliminary studies have shown that the region of *Fgf10* expression correlates with where motor neurons normally reside, which lead us to hypothesize that Fgf10 may be involved in the development of spinal motor neurons.

Hypothesis: Fgf10 is involved in the development of motor neurons

Aims: To investigate the hypothesis, three aims were set up:

1) To determine the timing and pattern of Fgf10 expression in the developing mouse spinal cord, across different embryonic ages.

2) To determine what cell types express Fgf10; are they motor neurons?

3) To investigate how loss of Fgf10 affects the development of motor neurons and other cell types in the spinal cord.

2. MATERIALS AND METHODS

2.1. Transgenic mouse lines

All mouse lines were bred on a mixed genetic background according to the local regulations for transgenic breeding.

2.1.1. *Fgf10*$^{LacZ/+}$ mice

Fgf10$^{LacZ/+}$ (*Fgf10-LacZ*) transgenic mouse line was originally created by Kelly in 2001 (Kelly et al., 2001). *Fgf10-LacZ* mice carry a heterozygous transgene insertion encoding nuclear *LacZ* (*nLacZ*) downstream of the *Fgf10* promoter and are acknowledged to be a reliable reporter of *Fgf10* expression (Hajihosseini et al., 2008; Kelly et al., 2001). The genomic structure of the *Fgf10-LacZ* allele is shown in Figure 2.1. *LacZ* gene encodes an enzyme β-galactosidase (β-gal), which in the presence of a substrate X-gal produces a blue precipitate. Therefore, *Fgf10* expression can be traced either by using anti- β-gal antibodies or by treating tissue with X-gal solution.

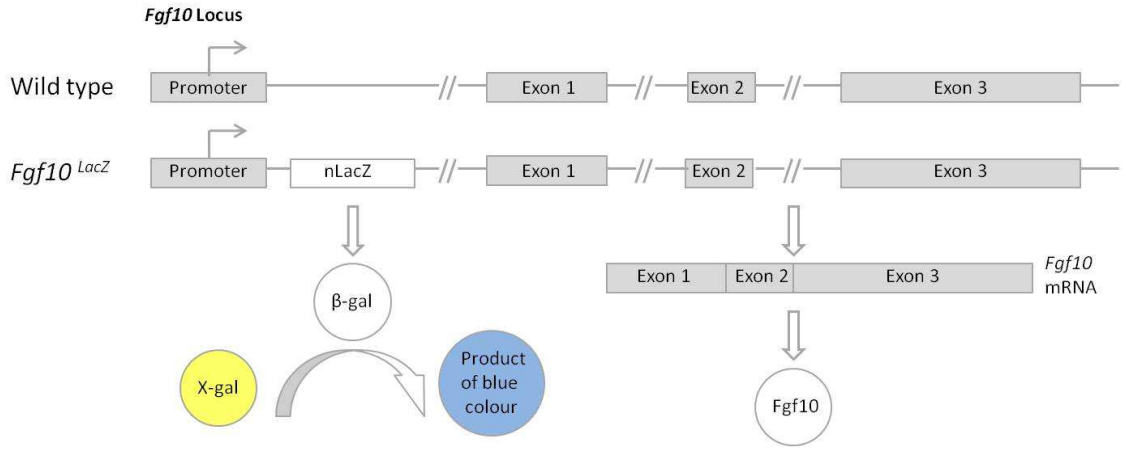

Fig. 2.1. Schematic diagram of the genomic structure of wild type (top) and *Fgf10-LacZ* (bottom) allele. The nuclear *LacZ* (*nLacZ*) transgene is located 114 bp upstream of the *Fgf10* gene and is under the control of the *Fgf10* promoter. LacZ gene encodes an enzyme β-galactosidase (β-gal), which converts substrate X-gal into a blue precipitate (Adapted from Kelly et al., 2001).

2.1.2. *Fgf10* $^{-/-}$ mice

Fgf10-/- (Fgf10 knockout) allele was originally generated by Min in 1998 (Min et al., 1998). A PGK-*neo* (NEO) cassette was inserted into the region of the first exon, which encodes the translation start site and the putative signal peptide. The genomic structure of the *Fgf10* knockout allele is shown in Figure 2.2. This strategy eliminated the translation initiation codon (ATG) and the signal peptide, and inserted multiple stop codons in-frame, as a result, no Fgf10 protein was produced. Homozygous *Fgf10* knockout mouse embryos (*Fgf10* $^{-/-}$) are smaller than wild type, they do not develop limbs and die at birth due to the absence of lungs (Fig. 2.3).

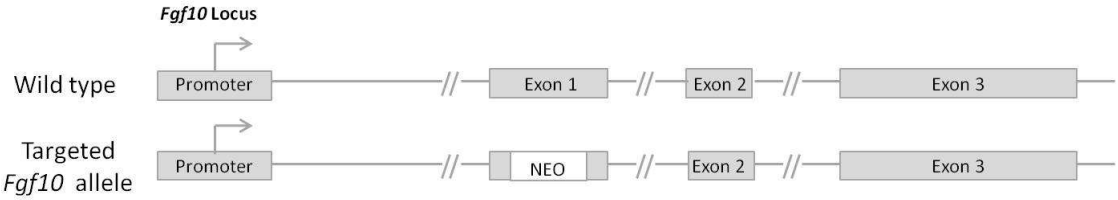

Fig. 2.2. Schematic diagram of the genomic structure of wild type (top) and *Fgf10* knockout (bottom) allele. A neomycin (NEO) cassette is inserted into the first axon of *Fgf10* gene that stops it from being transcribed (Adapted from Min et al., 1998).

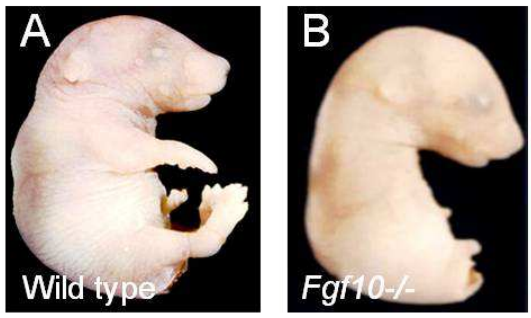

Fig. 2.3. Wild type (A) and *Fgf10* knockout (B) embryos at E18.5. Fgf10 knockout embryos lack limbs and lungs, and appear to be smaller in size compared to wild type (Adapted from Min et al., 1998).

2.1.3. *FgfR2-IIIc* $^{+/\Delta}$ mice

FgfR2-IIIc $^{+/\Delta}$ (*FgfR2-IIIc* hemizygotes) mice were originally generated by Hajihosseini in 2001 through a heterozygous *LoxP*-Cre mediated excision of "floxed" (flanked by *LoxP* sequences) exon 9, specific for FgfR2-IIIc isoform (Hajihosseini et al., 2001). For the genomic structure of the *FgfR2-IIIc* deficient allele, please, see Figure 2.4. Absence of one copy of *FgfR2-IIIc* in mice results in a gain-of-function effect due to a splicing switch in the *FgfR2-IIIc*

deficient allele. *FgfR2-IIIc* $^{+/\Delta}$ mice show illegitimate expression of FgfR2-IIIb isoform in mesenchymal and neural tissues along with FgfR2-IIIc. That makes the relevant tissues responsive not only to FgfR2-IIIc specific Fgfs (Fgf1, -2, -4, -6 and -9), but also to FgfR2-IIIb specific Fgfs (Fgf3, -7, -10 and -22). This leads to certain abnormalities, such as bone and visceral defects, which are reminiscent of Apert syndrome (Hajihosseini et al., 2001).

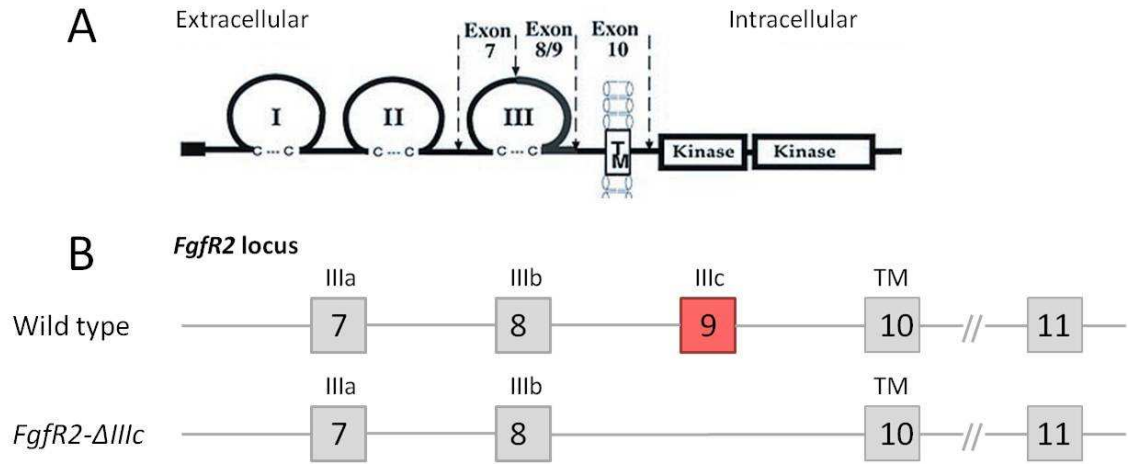

Figure 2.4. Structure of Fgf receptor and genomic structure of *FgfR2* locus in FgfR2-IIIc hemizygote mouse. (A) Schematic structure of FgfR2, which consists of an extracellular domain, containing three Ig-like loops, a transmembrane (TM) segment, and an intracellular tyrosine kinase domain. In the result of an alternative splicing of exons, encoding third Ig-like loop, either IIIb or IIIc receptor isoforms are generated. (B) Schematic diagram of the genomic structure of wild type (top) allele and *FgfR2* allele with excised exon 9 (bottom), that results in *FgfR2-IIIc* deficiency. Mice deficient in one copy of *FgfR2-IIIc* experience a gain-of-function mutation (Adapted from Hajihosseini et al., 2001).

2.2. Embryo isolation and genotyping

Animals were sacrificed by CO_2 asphyxiation, embryos of the relevant age (table 2.1) were isolated and their yolk sacs were harvested for genomic DNA isolation. Genomic DNA was isolated by digestion by Proteinase K overnight at 55°C, followed by sample centrifugation to remove the digested tissue. Genomic DNA was then precipitated with isopropanol and resuspended in 30% TE buffer in ddH_20. All embryos were genotyped by PCR using genomic DNA from embryo's yolk sacs. Embryos were genotyped by PCR using the Expand Long Template PCR System (Roche), according to manufacturer's instructions. For the list of primers used, please see table 2.2.

Genotype / Age	**Wild type**	***Fgf10*$^{LacZ/+}$**	***Fgf10*$^{-/-}$**	***FgfR2-IIIc*$^{+/\Delta}$**
E8.5	-	2	-	-
E9.5	3	5	-	-
E10.5	1	-	1	-
E11.5	-	7	-	-
E12.5	3	10	-	1
E14.5	1	1	1	-
E15.5	-	1	-	-

Table 2.1. Age, genotype and number of the embryos used in this study.

Allele	**Primers**	**Expected product/s (kbp)**
Fgf10^{lacZ}	(Forward) GCA TCG AGC TGG GTA ATA AGC GTT GGC AAT	*LacZ*+:0.8
	(Reverse) GAC ACC GAC ACA ACT GGT AAT GGT AGC GAC	
	(Forward) CGA GTG GAG CAT GTA CTT CCG TGT CCT GAA	Wild type: 0.5
	(Reverse) TCC CTA CCC AGT CAC AGT CAC AGC TGC ATA	
Fgf10 knockout	(Forward) CAC CAA AGA ACG GAG CCG GTTG	Knockout: 0.9
	(Reverse) ACT CTT TGG CCT CTA TCT AG	
FgfR2-IIIc $^{+/\Delta}$	(Forward) CAC TCT ATC AAG GCA TGC AGC AAGC	Floxed/+: 2.0 Wild type: 1.9
	(Reverse) CTG CGG CCG CCA GTC TGC CTG GCT CAC TGT CCT GCC	*FgfR2-IIIc* $^{+/\Delta}$ 0.5

Table 2.2. Primers used for genotyping (5'-3').

2.3. Tissue fixation

Embryos to be immunostained, were fixed with 4% paraformaldehide (PFA) at room temperature (RT) at least for 30 mins and then washed in PBS twice for 10 mins. Embryos to be treated with X-gal were fixed with 0.5% Gluteraldehyde and 2% PFA made in phosphate buffered saline (PBS), and then rinsed in PBS twice for 10 mins.

2.4. Dehydration and rehydration of the tissue

After fixation, embryos were dehydrated by being washed in PBS twice for 10 min, followed by washing in ascending series of ethanol, 30% and 50% ethanol made in PBS, 70% and 90% ethanol, made in dH_2O, each step being 15 to 30 min long, depending on the age of the embryos. Dehydrated embryos were stored in absolute ethanol at +4°C until use. Before sectioning, embryos were rehydrated to PBS by being washed in descending series of ethanol (90%, 70%, 50% and 30% ethanol), followed by washes in PBS, twice for 10 min.

2.5. X-gal staining

X-gal staining was performed to identify the presence of β-galactosidase. After fixation, the embryos were incubated at 37°C in pre-warmed 0.5 µg/ml X-gal, diluted in X-gal staining buffer (2 mM $MgCl_2$, 5 mM $K_4Fe(CN)_6$ and 5 mM $K_3Fe(CN)_6$ in PBS) for 2-4 hrs or overnight (o/n), until a blue precipitate was produced. The reaction was stopped by replacement of X-gal solution with PBS. The embryos were washed in PBS twice for 10 mins at RT on a rocking platform, followed by postfixation with 4% PFA for 15-30 mins and switched back to PBS by a 10 min wash. The embryos were then dehydrated and rehydrated in ascending and desceding series of ethanol respectively and sectioned on the vibratome.

2.6. Tissue blocking

Rehydrated embryos were immersed in molten solution of 3% agar (made in dH_2O) and placed into the water bath at +80°C for 15-20 min. Tubes containing embryos were agitated every 5 minutes for better agar penetration. The embryos and agar were then poured into tin-foil boats, the embryos were orientated into desirable position and the agar was allowed to set. Agar blocks were kept for 1 hour at RT to allow agar to set and then were stored at +4 °C overnight.

2.7. Tissue sectioning on the vibratome

The tissue was sectioned using a vibratome (microtome with vibrating blade) (Leica VT1000 S). Before sectioning, the foil was removed and excess agar was trimmed with a blade from the agar block, leaving a margin of about 0.5 cm around the embryo. The agar block was mounted onto the specimen disc using superglue, which was then inserted into the buffer tray. The buffer tray was filled with +4°C PBS, the blade was aligned and then sections were cut at 60-80 µm width. Sections were collected using a fine paint brush, transferred to wells of 48-well plates filled with PBS and stored at +4°C until used.

2.8. Immunostaining of vibratome sections

Immunostaining of vibratome sections was carried out in 3ml glass vials. To block non-specific binding sites, the sections were incubated at least for 2 hours at RT on a rocking platform, with solution containing 20% normal goat serum (NGS) and 1% Triton X100, diluted in PBS. After blocking, the sections were incubated at 4°C on a rocking platform with primary antibody diluted in a solution containing 0.2% NGS and 0.1% Triton X100, made in PBS (Table 2.3).

The next day, the sections were washed five times at RT on a rocking platform, each wash being an hour long, in 0.2% NGS and 0.1% Triron X100, prepared in PBS. The sections were then incubated o/n at 4°C on a rocking platform with the relevant secondary antibodies diluted in a solution containing 0.2% NGS and 0.5% NP-40, made in PBS (Table 2.4).

After incubation with a secondary antibody, the sections were washed six times in PBS at RT on a rocking platform, each wash being 30 mins long. During the last five minutes of the last wash sections were counterstained with Hoechst (1:1000), to visualize cell nuclei. The sections were then switched back to PBS by 10 mins wash and mounted onto the slides with an adhesive surface using Vectashield mounting medium (Vector Labs). Cover slips were put onto the slides and immobilized with clear nail varnish. Slides were stored at 4°C.

If a biotinylated secondary antibody was used the day before, the sections were washed five times at RT on a rocking platform, each wash being an hour long, in 0.2% NGS and 0.1% Triton X100, diltuted in PBS. The sections were then incubated at 4°C on a rocking platform with tertiary antibody diluted in 0.2% NGS and 0.5% NP-40, prepared in PBS (Table 2.5). The next day, the sections were washed in PBS, stained with Hoescht and mounted.

2.9. Immunostaining of tissue previously treated with X-gal

Before blocking non-specific binding sites, the sections were bleached for 1.5 hours at RT on a rocking platform, in a solution of 6% hydrogen peroxide, diluted from 30% stock solution and made in PBS. Then non-specific binding sites were blocked, sections were incubated with primary antibody and washed the next day as described above. The sections were then incubated o/n at 4°C on a rocking platform with a Goat anti-Rabbit Horse Radish Peroxidase (HRP) secondary antibody (1:1000) diluted in 0.2% NGS and 0.1% Triton X100, in PBS. The next day, the sections were washed 6 x 1 h in PBS, then 3 x 20 mins in 0.05M Tris-HCl buffer (0.1 M tris base, 0.1M HCl, ddH_2O, pH 8). Tris buffer was then replaced with chilled diaminobenzidine (DAB) staining solution (dH_2O, H_2O_2, Tris buffer, DAB). DAB staining was carried out and monitored under a dissecting microscope. After the stain became visible in the period from 30 sec to 2 mins, the reaction was stopped by replacing DAB staining solution with PBS. The sections were mounted as described above. All antibodies used in this study have been summarized in tables 2.3, 2.4 and 2.5.

Primary antibodies				
Antibody (anti-)	Raised in	Dilution	Cell type detected	Source
β-galactosidase	Rabbit	1:1000	product of bacterial gene, LacZ	Millipore (Chemicon)
β-galactosidase	Mouse	1:50-1:300	product of bacterial gene, LacZ	Sigma, Abcam, Cell Signalling, DSHB
BLBP	Rabbit	1:200	Radial glial cell marker	Abcam
GFAP	Rabbit	1:1000	Astrocytes	Chemicon (Millipore)
GFAP	Mouse	1:800	Astrocytes	Chemicon (Millipore)
Islet 1	Mouse	1:100	Differentiated motor neurons (except LMCl neurons)	DSHB
Lhx3	Rabbit	1:400	MMC neurons and V2 interneurons	Abcam
Nestin	Mouse	1:100	Neural precursors	DSHB
NeuN	Mouse	1:1500	Postmitotic neurons	Chemicon (Millipore)
Olig2	Rabbit	1:500	Oligo precursors	Chemicon (Millipore)
TuJ1	Mouse	1:1500	Differentiated neurons	Chemicon (Millipore)

Table 2.3. Primary antibodies used for immunostaining.

Secondary antibodies				
Antibody	**Raise**	**Conj**	**Diluti**	**Source**
mouse	Goat	Alexa 488	1:1000	Invitrogen
mouse	Goat	Alexa 568	1:1000	Invitrogen
rabbit	Goat	Alexa 488	1:1000	Invitrogen
rabbit	Goat	Alexa 568	1:1000	Invitrogen
mouse IgG	Goat	Biotinylated	1:300	Jackson Immunoresearch
mouse IgG1	Goat	Biotinylated	1:300	Jackson Immunoresearch
rabbit	Goat	HRP	1:1000	Vector Laboratories

Table 2.4. Secondary antibodies used for immunostaining.

Tertiary reagents		
Antibody (anti-)	**Dilution**	**Source**
Streptavidin-Texas-red	1:800	Jackson Immunoresearch

Table 2.5. Tertiary antibodies used for immunostaining.

2.10. Microscopy

Sections immunostained with fluorescent antibodies were imaged on a Zeiss Axioimager M2 microscope with an Apotome attachment. Sections immunostained with HRP antibody and/or stained with X-gal were imaged on an upright microscope using differential interference contrast (DIC). Images were acquired using Axiovision 4.8 software and processed using Adobe Photoshop. Cells in the sections were counted using Fiji software.

3. RESULTS

3.1 *Fgf10* is expressed in the ventral horns of the developing mouse spinal cord during neurogenesis

Previous unpublished studies from our laboratory have shown *Fgf10* expression in the developing mouse spinal cord at E12.5 by *in situ* hybridisation (Fig. 1.12). The first aim of my project was to examine the timing and pattern of *Fgf10* expression in the developing mouse spinal cord across different ages.

Presently, commercially-available anti-Fgf10 antibodies do not work well in immunohistochemical reactions, hence, *Fgf10-LacZ* mouse embryos were used. This mouse line carries a heterozygous *LacZ* transgene insertion downstream of *Fgf10* promoter (Kelly et al., 2001). *LacZ* gene codes for an enzyme β-galactosidase (β-gal), which converts substrate X-gal into a blue precipitate. In this mouse, β-gal has been shown to be a faithful reporter of Fgf10 expression (Kelly et al., 2001; Hajihosseini et al. 2008). However, it is not known how stable β-gal is, therefore, it might be detected not only in Fgf10 expressing cells, but also, in their descendants.

Embryos ranging from E8.5 to E15.5 were isolated from *Fgf10-LacZ* mice, treated with X-gal and *LacZ* positive embryos were sectioned on the vibratome in a transverse plane. Sections were mounted onto slides in the anatomical succession and imaged on an upright microscope with DIC filter.

It was found that β-gal positive (β-gal +) cells were present in the ventral region of the developing spinal cord from E 8.5 to E15.5 (Fig. 3.1 and 3.2). At E8.5 only one or two β-gal+ cells could be detected per section, and they were mainly located laterally in the spinal cord (Fig. 3.1). β-gal expressing cells were found in more rostral region, while in the caudal region of the spinal cord no β-gal positive cells were detected. These results suggested that Fgf10 expression started at E8.5 in the rostral region of the spinal cord.

At E9.5, β-gal+ cells were detected at all the levels of the spinal cord (Fig. 3.1). There were more β-gal+ cells than at E8.5, and organized in “bands” and restricted to the ventral region of the spinal cord. Consistent with β-gal expression pattern at E8.5, in the caudal part of the spinal cord there were less cells detected per section, than in the rostral part. These findings are consistant with downward displacement of cells in normal spinal cord development. Neurogenesis begins rostrally in the spinal cord and rostral part is more mature than caudal (Nornes and Carry, 1978).

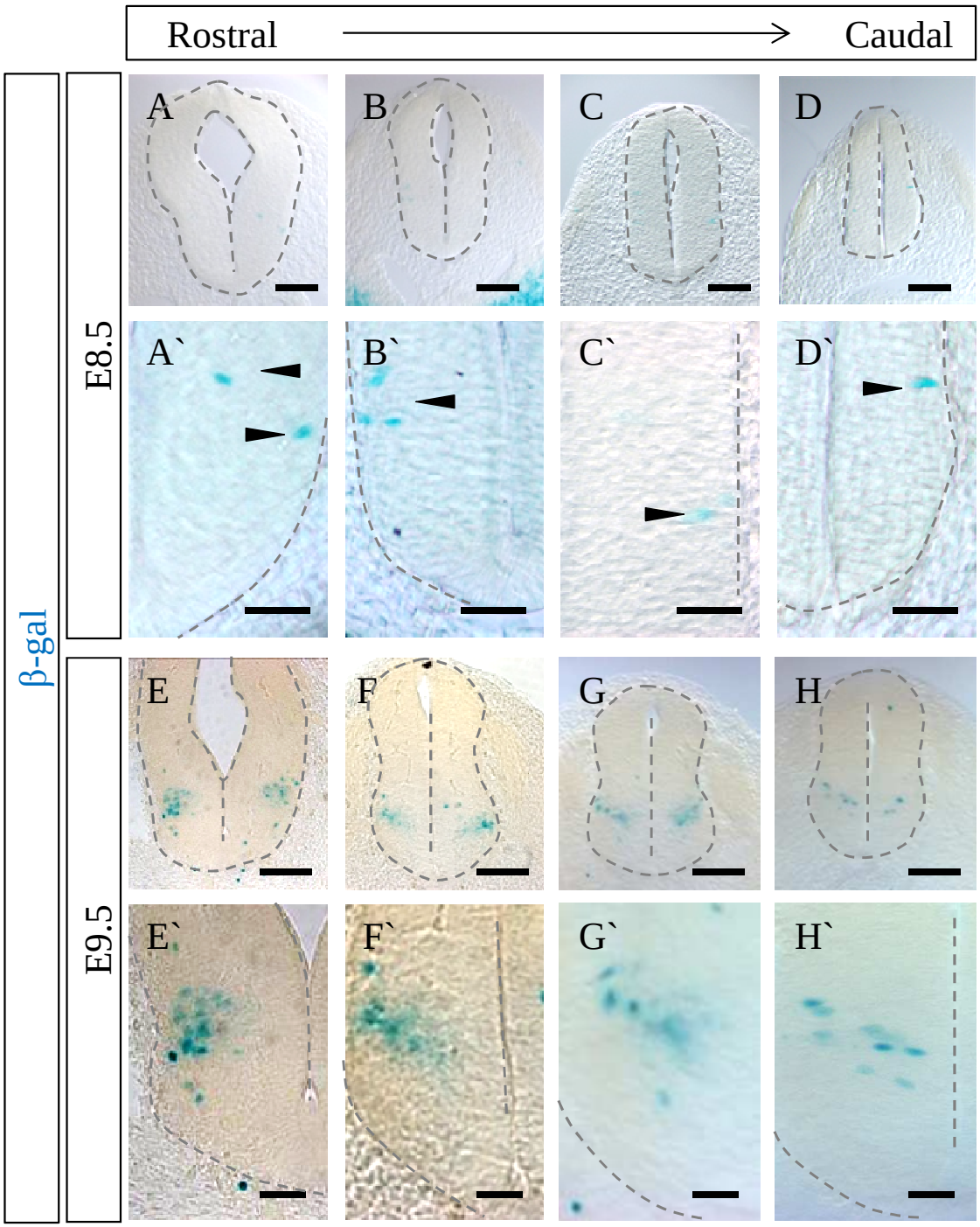

Fig. 3.1. Transverse sections of the spinal cord of E8.5 and E9.5 *Fgf10-LacZ* embryos treated with X-gal solution. X-gal is converted into a blue precipitate in the presence of an enzyme β-gal, encoded by *LacZ* gene. β-gal is a reporter of Fgf10 expression. At E8.5 (A – D`) there are a few β-gal positive cells (blue) per section, located laterally in the rostral region of the spinal cord. At E9.5 (E - H`) the number of β-gal positive cells increases and they can be detected throughout the whole spinal cord. Scale bars: (A-D; E-H) 100 µm; (A`-D`; E`-H`) 50 µm.

At E12.5, β-gal expression appeared to be present throughout the whole spinal cord, as at E9.5. However, at this stage β-gal+ cells were found clustered in the ventral horns of the spinal cord (Fig. 3.2).

At E14.5, β-gal expression pattern in the spinal cord changed, compared to E12.5 (Fig. 3.2). β-gal+ cells were still located in the ventral horns of the spinal cord at more rostral regions, but also, new zones of β-gal expressing cells emerged in the dorsal region of the spinal cord, on either side of the ventricular zone. By E14.5 β-gal expression was discontinued in the caudal region of the spinal cord.

At E15.5, β-gal expression pattern was very similar to E14.5 (Fig. 3.2).

Knowing that β-gal is a reliable reporter of Fgf10 expression, these results suggested that Fgf10 expression started at E8.5 in the rostral region of the spinal cord, continued during E9.5 to 14.5 throughout the whole spinal cord in the ventral horns and expired from the caudal part of the spinal cord by E14.5. At least from E14.5 new zones of Fgf10 expression emerged in more rostral part in the dorsal region of the spinal cord close to the ventricular zone.

Pattern of β-gal expression in the developing spinal cord of *Fgf10-LacZ* mice has been summarized in a schematic diagram (Fig. 3.3). Timing of β-gal and, therefore, Fgf10 expression appeared to correlate with the period of neurogenesis in the spinal cord and its expression pattern resembled the location of motor neuron bodies during spinal cord development. Consequently, the next step was to determine the exact phenotype of Fgf10 expressing cells or their descendants in the developing spinal cord.

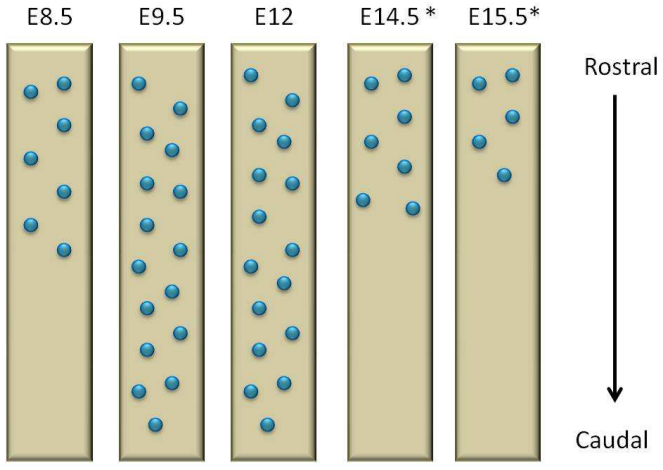

Figure 3.3. Schematic diagram of β-gal expression in the developing spinal cord of *Fgf10-LacZ* reporter mouse from E8.5 to E15.5. At E8.5 β-gal is expressed in the rostral region of the spinal cord. At E9.5 to E12 β-gal is present throughout the whole spinal cord. At E 14.5 and E15.5 β-gal expression is present rostrally. Please, note, that β-gal is expressed in the ventral region of the spinal cord, unless otherwise noted. Asterics (*) indicates that β-gal is expressed in the ventral and dorsal regions of the spinal cord.

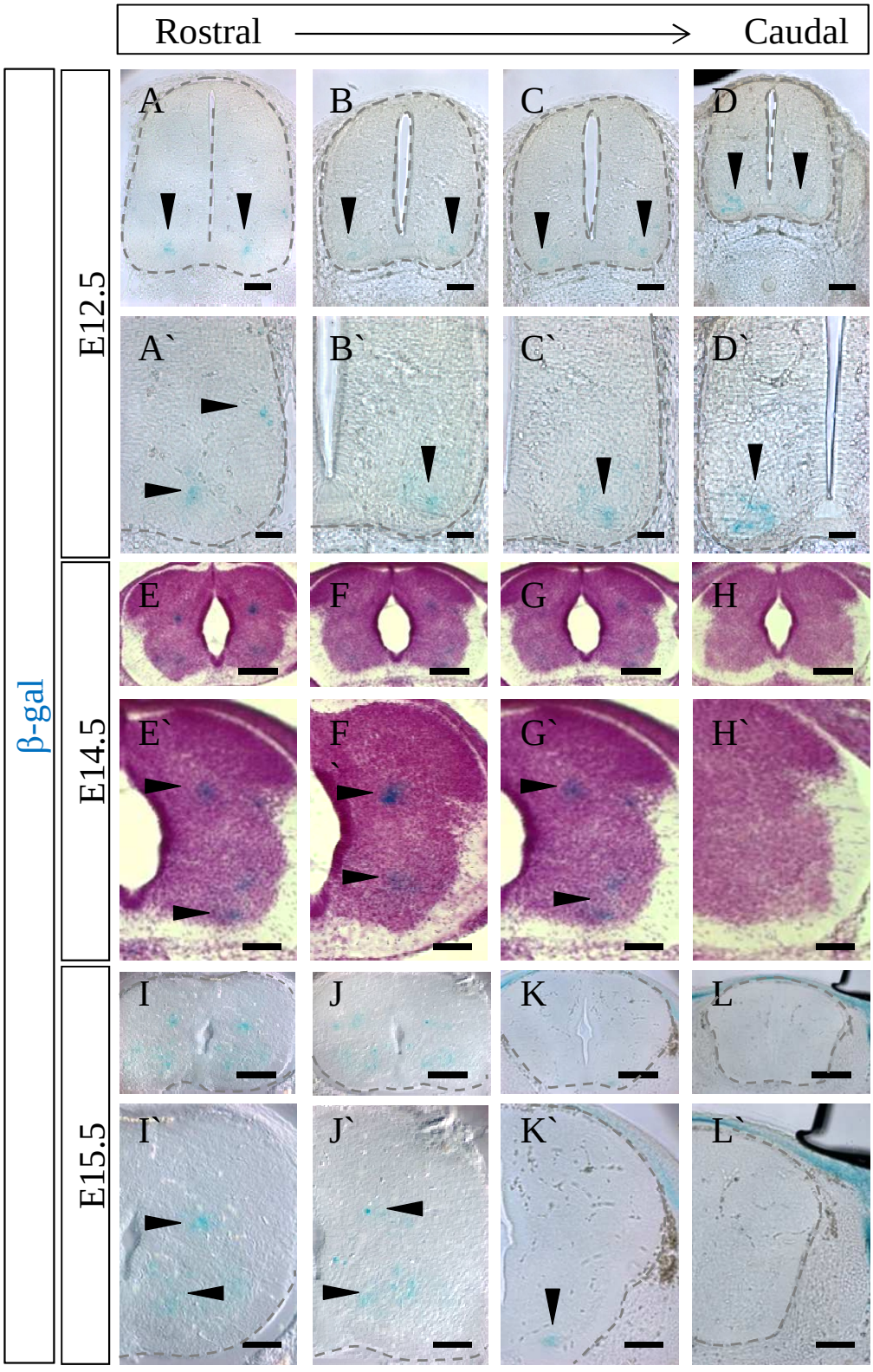

Fig. 3.2. Transverse sections of the spinal cord of E12.5, E14.5 and E15.5 *Fgf10-LacZ* embryos treated with X-gal solution. X-gal is converted into a blue precipitate in the presence of an enzyme β-gal, encoded by *LacZ* gene. β-gal is a reporter of Fgf10 expression. At E12.5 (A – D`) β-gal positive cells (blue) are present throughout the whole spinal cord and are located in the ventral horns. At E14.5 (E – H`) β-gal expression expires from caudal region, while in the rostral region it is present in the ventral horns and a new area of β-gal expression emerges in dorsal part of the spinal cord on either side, close to the ventricular zone. At E15.5 (I – L`) pattern of β-gal expression is very similar to the one at E14.5. Scale bars: (E-H; I-L) 200 µm; (A-D; E`-H`; I`-L`) 100 µm; (A`-D`) 50 µm.

3.2 Fgf10 is expressed by a subset of spinal motor neurons from the early stage of their differentiation

3.2.1. Rb-anti-β-gal provides specific staining in the developing spinal cord of *Fgf10-LacZ* mice

In order to determine what cell types express β-gal, I investigated potential colocalization of anti-β-galactosidase antibody (anti-β-gal) with various neuronal markers using double-immunostaining technique. Double-immunostaining requires that primary antibodies are raised in different species. Given that primary antibodies against neuronal markers, we were interested in, were raised in rabbit (Lhx3) and in mouse (NeuN and Islet1, TuJ1), both anti-β-gal antibodies (rabbit-anti-β-gal and mouse-anti-β-gal) were needed to examine potential coexpression of β-gal with each neuronal marker.

First, sections of the spinal cord at E9.5 were immunostained with different anti-β-gal antibodies to show that β-gal could be detected by immunohistochemistry. Embryos were isolated from *Fgf10-lacZ* mouse, genotyped for the presence of *LacZ* gene and then *LacZ* positive embryos were sectioned in a transverse plane. Sections of a brain derived from *LacZ* positive adult mouse were used as a positive control (K+) for the tissue, because it was shown previously to contain areas of β-gal expression, e.g. in hypothalamus and hipoccampus (Hajihosseini et al., 2008). Spinal cord and brain sections were then immunostained with anti-β-gal, raised in rabbit or in mouse, and imaged on Zeiss Axioimager M2 microscope with an Apotome attachment.

Immunostaining with rabbit-anti-β-gal (rb-anti-β-gal) provided specific staining both in the K+ and in the spinal cord sections, while none of mouse-anti-β-gal (ms-anti-β-gal) antibodies worked. Four ms-anti-β-gal antibodies (Abcam, Sigma, Cell Signalling and Developmental Studies Hybridoma Bank) were used under different conditions and in various concentrations, but all of them failed to provide any staining.

The pattern of β-gal expression at E9.5 provided by immunostaining was consistent with the one detected in tissue treated with X-gal, although, in immunostained sections there were less β-gal expressing cells per section compared to X-galled tissue (Fig 3.1 and 3.4). This could be explained by the fact that β-gal expressing cells are lying on different levels within the section and it was not possible to image all β-gal+ cells at once in immunostained tissue, because some would be out of the plane of focus. Thus, X-gal solution could be more sensitive, than anti-β-gal antibody.

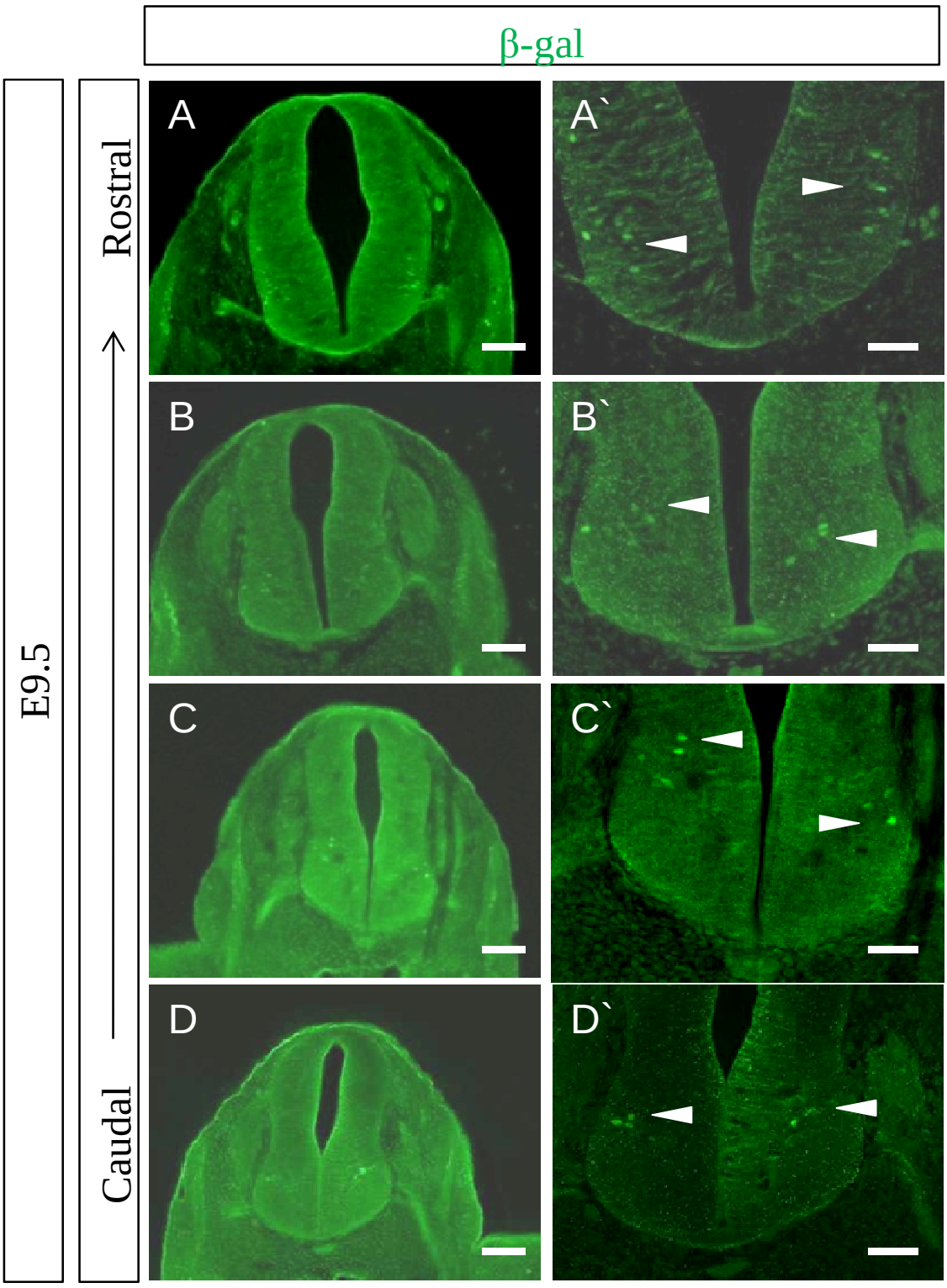

Fig. 3.4. Transverse sections of the spinal cord of E9.5 *Fgf10-LacZ* embryo immunostained with rb- anti-β-gal antibody. β-gal (green) is a reporter of Fgf10 expression. β-gal positive cells can be detected throughout the whole spinal cord. The pattern of β-gal expression detected by immunostaining is consistent with the one detected by X-gal solution. Scale bars: (A-D) 100 µm; (A`-D`) 50 µm.

These results suggested that rb-anti-β-gal antibody provided specific staining and could be used in double-immunostaining in combination with antibodies raised in mouse, while ms-anti-β-gal antibodies could not be employed in this study. In order to investigate potential coexpression of β-gal with those neuronal markers, antibodies against which were raised in rabbit, staining with Horse Radish Peroxidase (HRP) was employed. X-gal stained tissue was immunostained with relevant primary antibody and then with secondary HRP antibody, the colour was developed using DAB staining solution.

3.2.2. Motor neuron and oligodendrocyte *progenitors* do not express Fgf10 in the developing mouse spinal cord

Previously, it was shown that β-gal expression in the spinal cord starts at the beginning of neurogenesis at E9.5. To see if β-gal is expressed in the ventricular zone cells (VZ cells), sections of *LacZ* positive embryos aged E9.5 were immunostained with rb-anti- β-gal and rb-Olig2 antibody. At E9.5 Olig2 is a marker of both motor neuron and oligodendrocyte progenitors; oligodendrocytes are generated later at E12.5-13.

As β-gal and Olig2 (rb-Olig2) antibodies were both raised in rabbit and could not be used together for double-immunostaining, adjacent sections were immunostained with each antibody separately (Fig. 3.5). Analysis showed that β-gal expressing cells lie within the domain of MN/OL progenitors and possibly coexpress Olig2.

To see if it was the case, sections of X-gal stained embryos at E9.5 were stained with rb-Olig2 and HRP secondary antibody, and colour was then developed using DAB staining solution (Fig. 3.6). Sections were imaged using upright microscope with DIC filter. Consistently with previous results, β-gal+ cells lay within the Olig2 domain, however, they did not appear to coexpress Olig2. In more rostral region of the spinal cord the number of β-gal+ cells increased, and more of them were lying out of Olig2 domain.

These results suggested that Fgf10 was not expressed in motor neuron and oligodendrocyte *progenitors*.

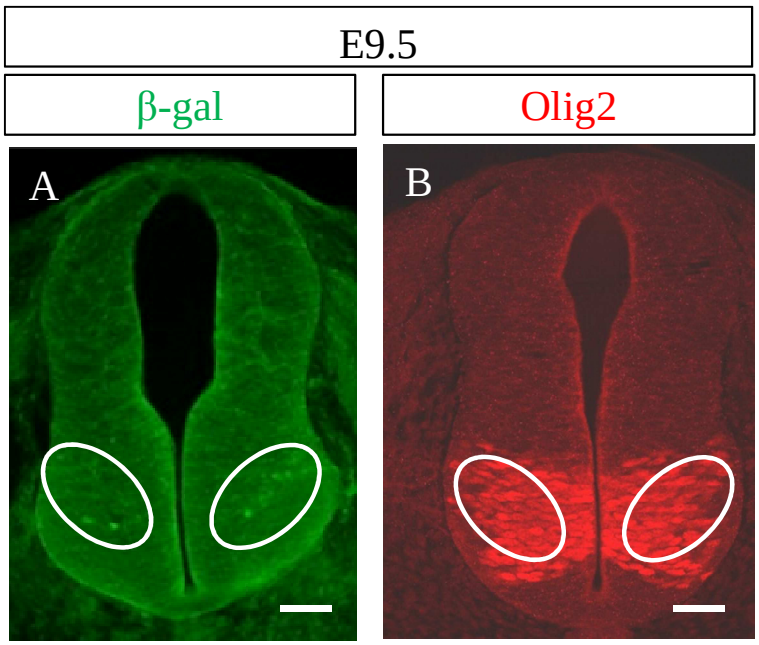

Fig. 3.5. Transverse sections of the spinal cord of E9.5 *Fgf10-LacZ* embryo immunostained with rb-anti- β-gal (A) and rb-Olig2 (B) antibodies. β-gal (green) is a reporter of Fgf10 expression, while Olig2 (red) marks motor neuron and oligodendrocyte progenitors. Domain of β-gal positive cells appears to correlate with the domain of motor neuron and oligodendrocyte progenitors. Scale bars: (A, B) 50 µm.

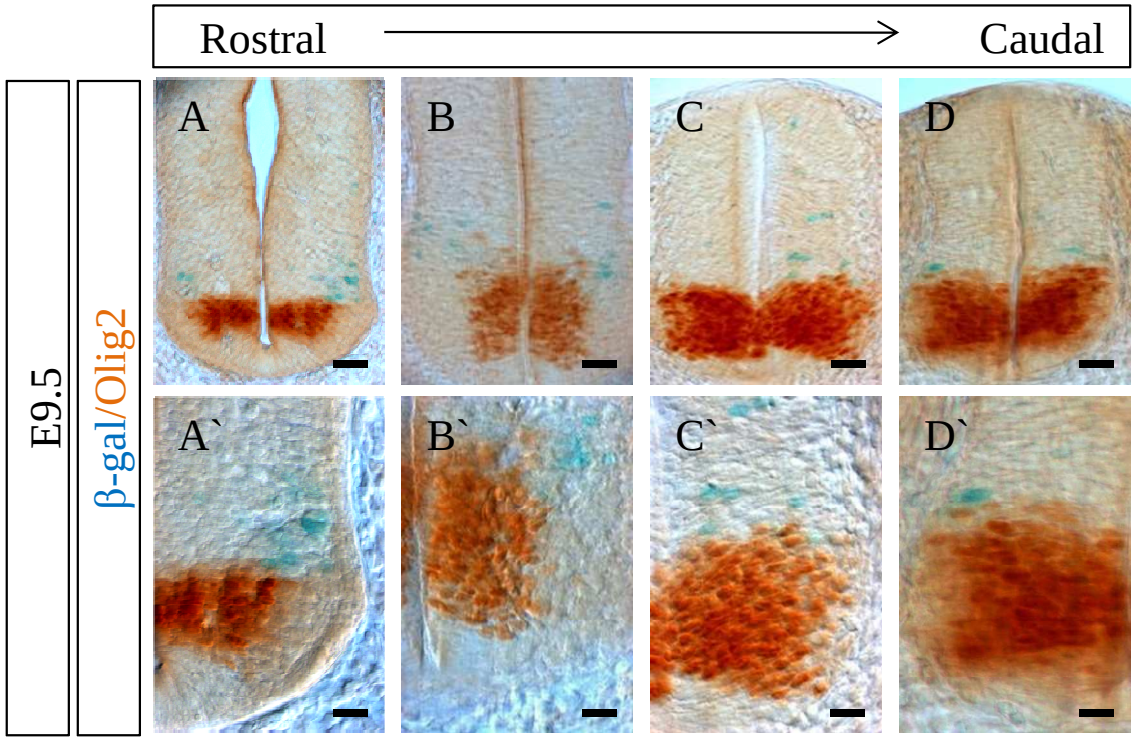

Fig. 3.6. Transverse sections of the spinal cord of X-galled E9.5 *Fgf10-lacZ* embryo stained with rb-Olig2 and Horseradish Peroxidase. β-gal (blue) converts X-gal to a product of blue color, and is a reporter of Fgf10 expression. Olig2 marks motor neuron and oligodendrocyte progenitors. β-gal positive cells lie within Olig2 domain, although β-gal expression does not colocalize with Olig2 expression. In more rostral sections more β-gal positive cells lie out of Olig2 domain. Scale bars: (A-D) 50 µm; (A`-D`) 25 µm.

3.2.3. A subset of differentiated neurons expresses Fgf10 in the developing mouse spinal cord

As β-gal expression appeared to be absent from VZ cells, but still was located very close to the progenitor domain, there was a high possibility that it would be expressed in differentiating neurons.

To see if β-gal was expressed in neurons, double-immunostaining was performed using rb-anti-β-gal antibody and TuJ1 (Neuron-specific class III β-tubulin) antibody raised in mouse (ms-TuJ1), that is expressed in neurons in CNS and PNS from the early stage of neural differentiation and onwards. Transverse sections of E9.5 *LacZ* positive embryos were double-immunostained and imaged using Zeiss Axioimager M2 microscope with an Apotome attachment. It was shown that all β-gal+ cells expressed TuJ1 (Fig. 3.7).

However, immunostaining with TuJ1 antibody did not allow to distinguish between early born neurons and more mature ones. In order to understand if Fgf10 was expressed in postmitotic neurons, NeuN antibody raised in mouse (ms-NeuN), a marker of postmitotic neurons, was used in double-immunostaining in combination with rb-anti-β-gal.

According to the literature, all neurons migrate out of the ventricular zone when they exit their cell cycle (Wolpert et al., 2007). However, not all the neurons outside ventricular zone were positive for a marker of postmitotic neurons, i.e. NeuN. That suggests that NeuN is expressed in more mature neurons, and those which lack NeuN expression are in the early stage of differentiation. It was shown that β-gal expression colocalized with a subset of NeuN expressing cells, although there were β-gal expressing cells that did not express NeuN (fig. 3.8).

β-gal expression and, therefore, Fgf10 expression, was detected in a subset of neurons at the early stage of differentiation, as well as in a subset of postmitotic neurons. However, one would have to take into consideration that anti-β-gal antibody could be labelling Fgf10+ cells and/or their descendants.

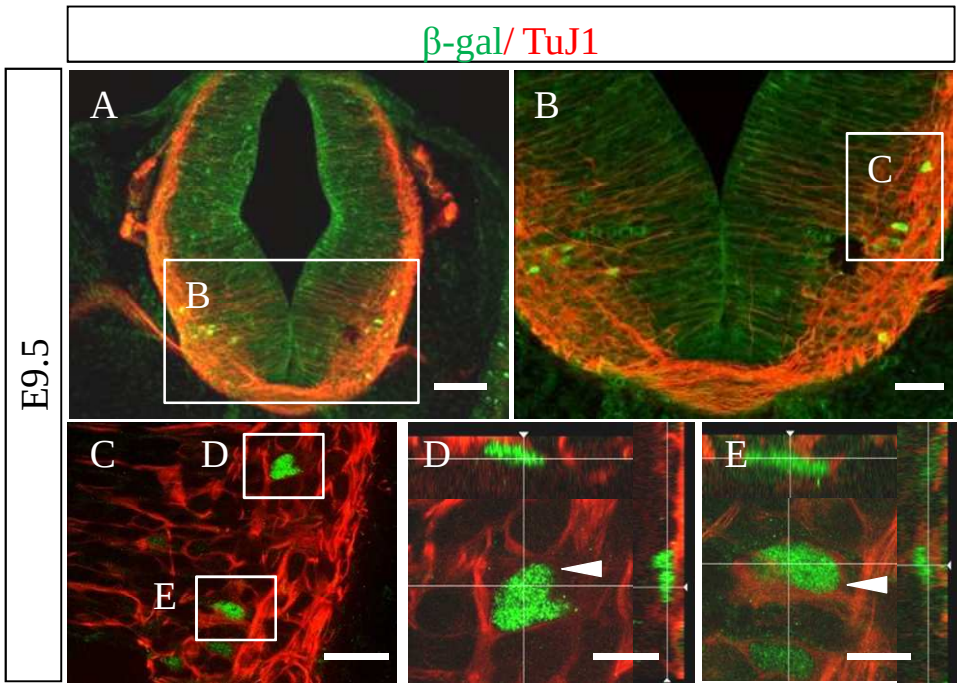

Fig. 3.7. Transverse sections of the spinal cord of E9.5 *Fgf10-LacZ* embryo immunostained with rb-anti- β-gal and anti- ms-TuJ1. β-gal (green) is a reporter of Fgf10 expression and TuJ1(red) marks neurons from the early stage of their differentiation and onwards. β-gal expression colocolizes with TuJ1 expression. Scale bars: (A) 100 µm; (B) 50 µm; (C) 25 µm; (D, E) 10 µm.

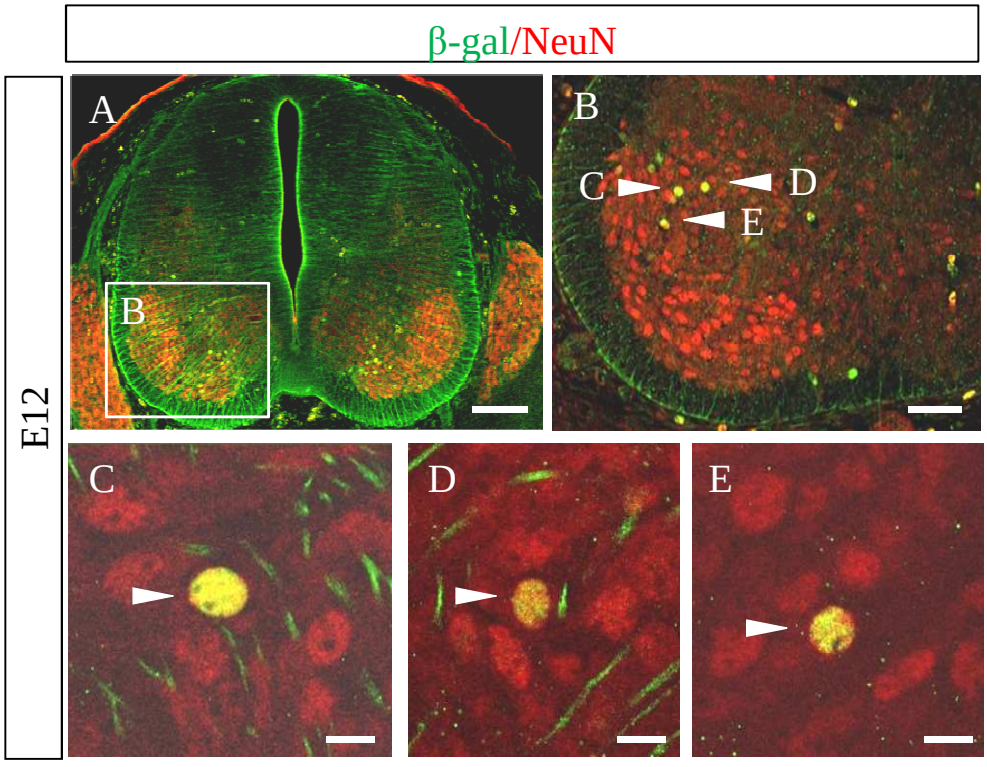

Fig. 3.8. Transverse sections of the spinal cord of E12 *Fgf10-LacZ* embryo immunostained with rb-anti- β-gal and anti- ms-NeuN. β-gal (green) is a reporter of Fgf10 expression and NeuN(red) marks postmitotic neurons. A subset of NeuN positive cells express β-gal. Scale bars: (A) 100 µm; (B) 50 µm; (C, D, E) 10 µm.

3.2.4. A subset of motor neurons expresses Fgf10 in the developing mouse spinal cord

Fgf10 was shown to be expressed by differentiated neurons and the pattern of its expression, as discussed previously, “mimicked” the location of motor neurons in the spinal cord. To see if Fgf10 was expressed in motor neurons, double-immunostaining was performed using rb-anti-β-gal antibody and motor neuron markers Islet1 and Lhx3. Islet1 is a LIM-homeodomain protein initially expressed in all motor neurons immediately after they exit the mitotic cycle, but later it is restricted to specific motor neuron subtypes (MMC, HMC, PGC and LMCm), while Lhx3 is a marker of MMC neurons and V2 interneurons.

Initially, staining with anti-Islet1 antibody raised in mouse (ms-Islet1) was perfomed on sections of *LacZ* positive embryos aged E9.5, while sections of older embryos (E12) were used as a K+. Ms-Islet1 provided specific staining in the spinal cord at E12, however no specific staining was detected in sections of embryos aged E9.5 (data not shown). The reason could be that it was too early for Islet1 to be expressed at E9.5, yet. Consequently, sections of E12 embryos were used for immunostaining with motor neuron markers.

Double-immunostaining with rb-anti-β-gal and ms-Islet1 was performed on sections of *LacZ* positive embryos and imaged. It was found that some, but not all β-gal+ cells coexpressed Islet 1 (Fig. 3.9).

These results showed that Fgf10 was expressed by a subset of motor neurons that expressed Islet1, i.e. all neuronal subtypes except LMCl.

Lhx3 antibody was raised in rabbit (rb-Lhx3), hence staining with HRP on X-galed embryonic tissue was employed. Sections of E12 embryos treated with X-gal were stained with rb-Lhx3 and HRP secondary antibody, and colour was then developed by DAB staining solution. Sections were imaged using an upright microscope with DIC filter. β-gal+ cells were mainly located in the ventral horns of the spinal cord, where MMC neurons normally reside. Some, but not all β-gal+ cells coexpressed Lhx3 (Fig. 3.10).

Acquired results suggested that Fgf10 was expressed by a subset of MMC neurons.

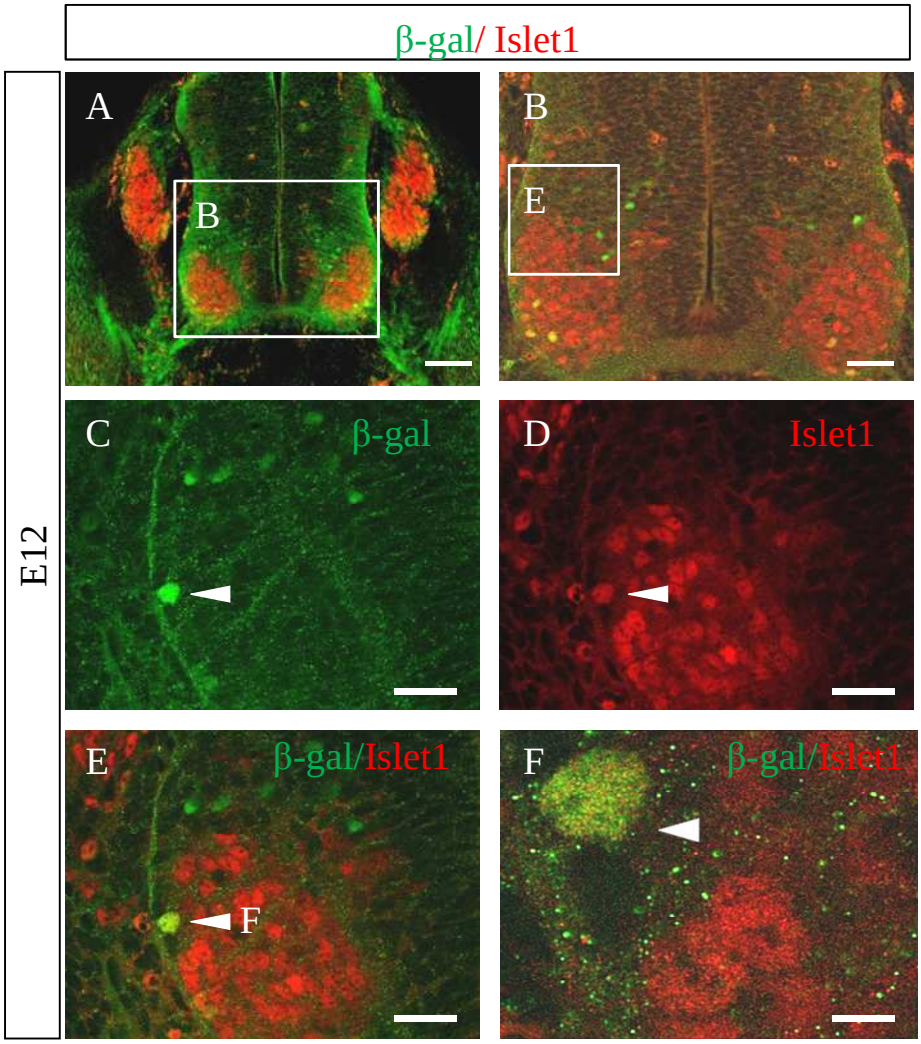

Fig. 3.9. Transverse sections of the spinal cord of E12 *Fgf10-LacZ* embryo immunostained with rb-anti- β-gal and anti- ms-Islet1. β-gal (green) is a reporter of Fgf10 expression and Islet1(red) marks all motor neurons, except LMCl neurons. A subset of Islet1 positive cells express β-gal. Scale bars: (A) 100 µm; (B) 50 µm; (C, D, E)25 µm; (F) 5 µm.

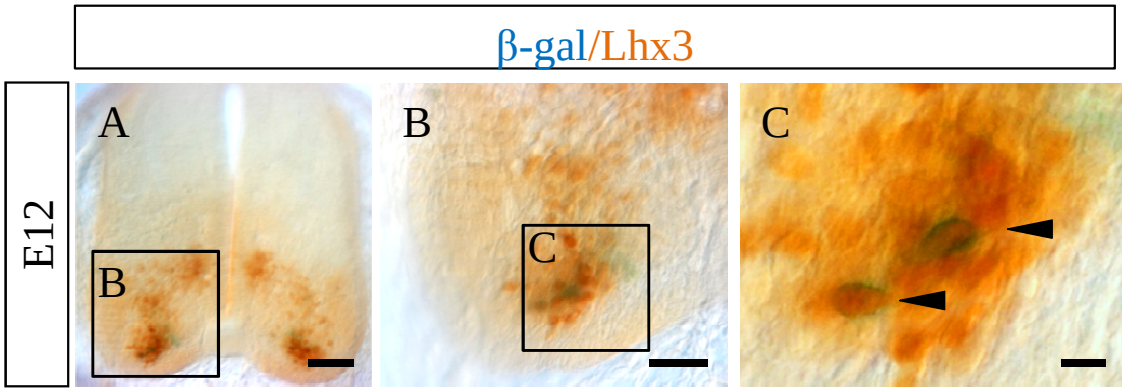

Fig. 3.10. Transverse sections of the spinal cord of X-gal stained E12 *Fgf10-LacZ* embryo stained with rb-Lhx3 and Horseradish Peroxidase. β-gal (blue)converts X-gal into a product of blue colour and is a reporter of Fgf10 expression. Lhx3 marks neurons of medial motor column and V2 interneurons. A subset of Lhx3 positive cells express β-gal. Scale bars: (A) 100 µm; (B) 50 µm; (C) 10 µm.

3.3. Functional analysis of Fgf10 in the developing spinal cord of *Fgf10* knockout mice

Fgf10 was shown to be expressed in spinal motor neurons during neurogenesis. Therefore, it might have a role in motor neuron development, which includes MN migration, differentiation into particular subtypes, segregation into motor columns, axon projections, synapsing and MN survival during cell death.

To investigate the role of Fgf10 in the development of spinal motor neurons, *Fgf10* knockout mice were used (Min et al., 1998). The genome of *Fgf10* knockouts contains a PGK-*neo* cassette inserted into the region of the first exon of *Fgf10* that encodes the transcription initiation site and the putative signal peptide. This results in disruption of the translation initiation codon (ATG), thus, no functional Fgf10 protein being produced. Homozygous *Fgf10* knockout mouse embryos (*Fgf10* $^{-/-}$) are smaller than wild type, do not develop limbs, and die at birth due to the absence of lungs (Fig. 2.3).

Fgf10 knockout and wild type embryos were sectioned in a transverse plane, comparable sections of the same level were then chosen (based on spinal cord and ventricular shape), immunostained and imaged. Sections of *Fgf10* knockout and wild type embryos at E10.5 and E14.5 were immunostained with various neuronal and glial markers e.g. Lhx3, NeuN, Islet1, Olig2, and compared to elucidate potential variation between them.

3.3.1. Loss of Fgf10 does not appear to affect spinal motor neurons at the beginning of neurogenesis

Fgf10 expression was shown to begin at E8.5, hence, to see if Fgf10 played a crucial role in the beginning of neurogenesis, immunostaining was performed on embryos aged E10.5. Sections of *Fgf10* knockout and wild type embryos were immunostained with ms-NeuN in order to see potential differences in number or location of postmitotic neurons, as well as with rb-Lhx3 to see if there were any differences in MMC neurons and V2 interneurons in particular.

There were no obvious differences in the pattern of NeuN expression between *Fgf10* knockouts and wild type embryos at E10.5 (Fig. 3.11).

Lhx3 expression pattern in *Fgf10* knockout and wild type embryos was very similar. On gross examination it seemed that in *Fgf10* knockouts there were more Lhx3 positive (Lhx3+) cells than in wild type. Lhx3+ cells were counted in 8 representative sections and numbers were compared between sections of the same level in wild type and *Fgf10* knockout embryos (Table 3.1). However, it appeared that the number of Lhx3+ cells per section did not differ significantly in the comparable sections of wild type and Fgf10 knockout embryos (Fig. 3.12).

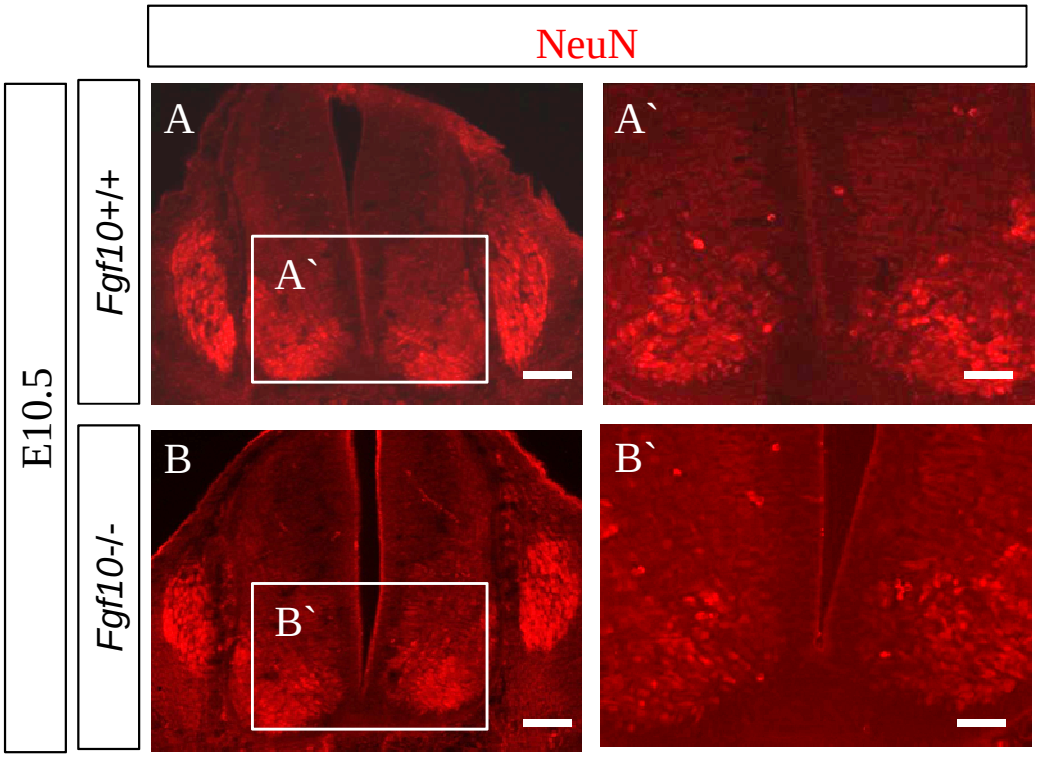

Fig. 3.11. Transverse sections of the spinal cord of wild type and Fgf10 knockout embryos at E10.5 immunostained with ms-NeuN. NeuN marks postmitotic neurons. Loss of Fgf10 expression does not appear to affect pattern of NeuN expression. Scale bars: (A, B) 100 µm; (A`,B`) 50 µm.

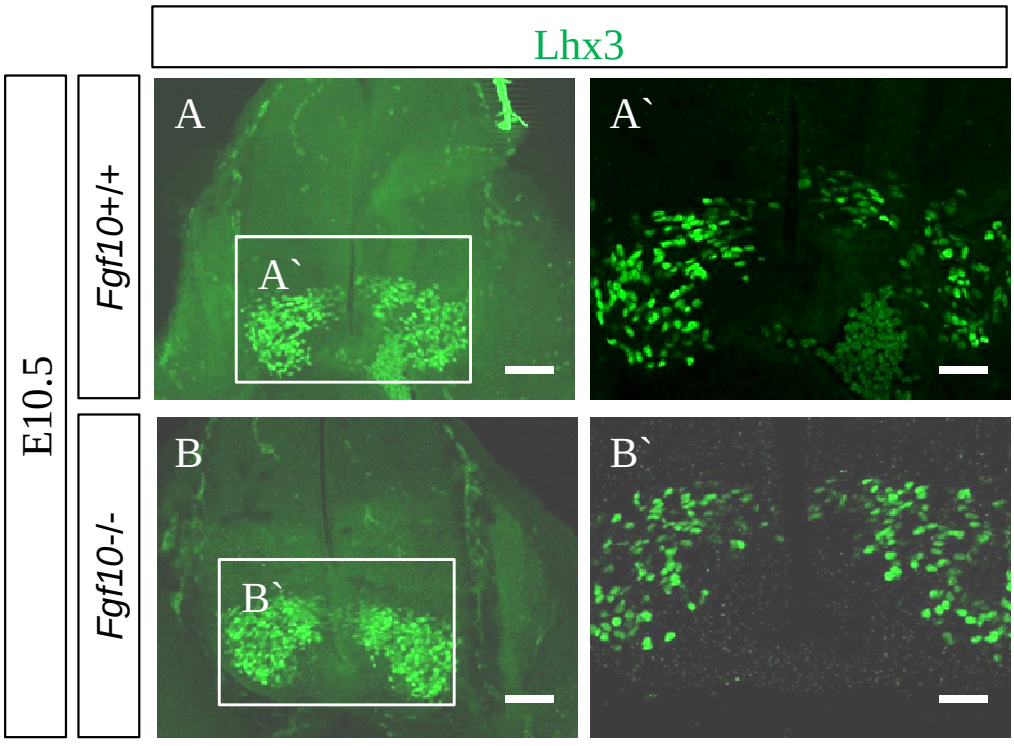

Fig. 3.12. Transverse sections of the spinal cord of wild type and Fgf10 knockout embryos at E10.5 immunostained with rb-Lhx3. Lhx3 marks neurons of medial motor column and V2 interneurons. Loss of Fgf10 expression does not appear to affect pattern of Lhx3 expression. Scale bars: (A, B) 100 µm; (A`,B`) 50 µm.

Section №	1	2	3	4
Wild type	144	150	164	83
***Fgf10* -/-**	140	154	166	85

Table 3.1. Amount of Lhx3 positive cells per section in the transverse plane (width 70 µm) in wild type and *Fgf10* knockout embryos aged E10.5.

Obtained results suggested that at the beginning of neurogenesis loss of Fgf10 expression did not drastically affect time of neuronal differentiation i.e. timing of NeuN expression, the number of MMC neurons and V2 interneurons and migration of neurons.

3.3.2. Loss of Fgf10 expression does not appear to affect motor neuron and oligodendrocyte progenitors at the beginning of neurogenesis

Fgf10 is a signalling molecule and at E9.5 it was shown to be expressed in cells lying within or very close to domain of motor neuron and oligodendrocyte progenitors. Consequently, it could play a role in the development of neural progenitors.

To see if there was any difference in neural progenitor pattern in the spinal cords of *Fgf10* knockout and wild type embryos, comparable sections of *Fgf10*-/- and wild type embryos aged E10.5 were immunostained with Olig2, a marker of motor neuron and oligodendrocyte progenitors. The pattern of Olig2 positive (Olig2+) cells appeared to be similar in *Fgf10* knockout and wild type embryos (Fig. 3.13). Olig2+ cells were counted in four representative sections and the number of Olig2+ cells in Fgf10 knockouts was very close to their number in wild type (Table 3.2).

Section № / Genotype	1	2
Wild type	34	33
***Fgf10* -/-**	35	33

Table 3.2. Amount of Olig2 positive cells per section in the transverse plane (width 70 µm) in wild type and *Fgf10* knockout embryos aged E10.5.

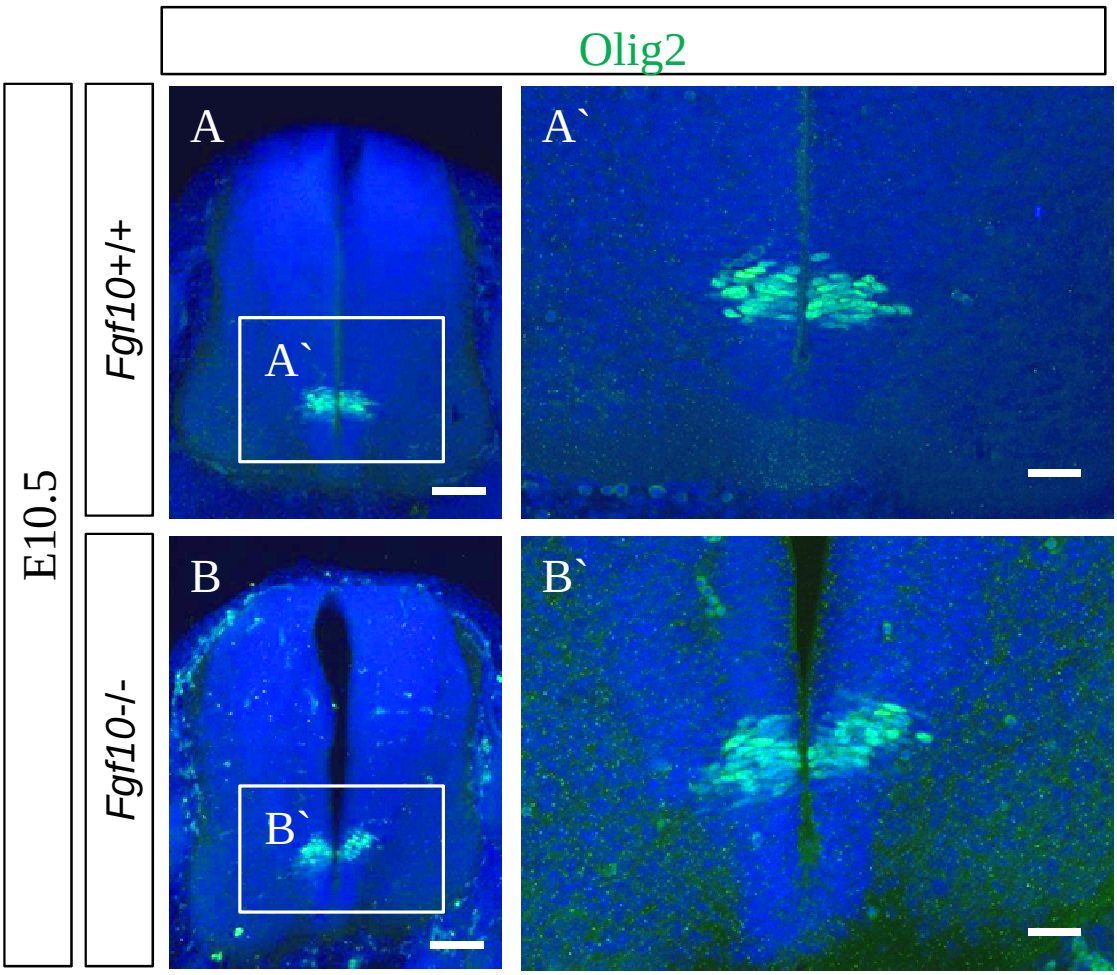

Fig. 3.13. Transverse sections of the spinal cord of wild type and Fgf10 knockout embryos at E10.5 immunostained with rb-Olig2 and counterstained with Hoechst. Olig2 (green) marks motor neuron and oligodendrocyte progenitors; Hoechst marks cell nuclei. Loss of Fgf10 expression does not appear to affect number and pattern of Olig2 + cells. Scale bars: (A, B) 100 µm; (A`,B`) 50 µm.

Achieved results suggested that Fgf10 expression was not necessary for regulating the number and position of motor neuron and oligodendrocyte progenitor cells at the beginning of neurogenesis.

3.3.3. Loss of Fgf10 does not appear to affect oligodendrocytes and spinal motor neurons at the end of neurogenesis

Fgf10 loss did not appear to affect MMC neurons and V2 interneurons, as well as MN/OL progenitors at the beginning of neurogenesis. However, according to β–gal expression detected in the developing mouse spinal cord from E8.5 to E15.5, it might be too early for the consequences of Fgf10 loss to become obvious at E10.5. Hence, *Fgf10* knockout and wild type spinal cord sections were compared at E14.5, when β–gal expression disappears from the caudal

region of the spinal cord. By that time, normally most of spinal motor neurons are born and segregated into motor columns.

Comparable transverse sections of *Fgf10* knockouts and wild type embryos were immunostained with various neuronal (NeuN, Islet1, Lhx3) and glial cell (Olig2) markers. Olig2 at this stage is a marker of oligodendrocytes progenitors and precursors.

The expression patterns of NeuN, Islet1 and Olig2 in the spinal cord of *Fgf10* knockout were similar to wild type and no major differences could be detected (Fig. 3.14).

However, there seemed to be a difference in Lhx3 expression pattern (Fig. 3.15). In *Fgf10* knockouts, the number of Lhx3+ cells located in the ventral horns of the spinal cord and making up medial motor column seemed to be higher, than in wild type. Cell counting showed that the number of Lhx3+ cells in the ventral horns per 50 µm was the same in wild type and in *Fgf10* knockout embryos (Table 3.3). Although, the number of neurons turned out to be the same, Lhx3+ motor neurons appeared to be more dispersed in *Fgf10* knockouts. This could have been a reason for assumption that there were more of them in Fgf10 knockouts, than in wild type.

Section № / Genotype	**1**	**2**	**3**	**4**
Wild type	23	18	16	13
***Fgf10* -/-**	21	20	16	12

Table 3.3. Amount of Lhx3 positive cells per section in the transverse plane (width 50 µm) in wild type and *Fgf10* knockout embryos aged E14.5. Please note that not all Lhx3+ cells were counted per section, but only Lhx3+ cells clustered in a column in one of the ventral horns of the spinal cord.

Obtained results suggested that Fgf10 loss did not affect generation and maturation of Lhx3+ neurons in the spinal cord, as there was no obvious difference between NeuN expression patterns in *Fgf10* knockout and wild type embryos. Oligodendrocyte generation and distribution did not seem to be affected by Fgf10`s absence, either. Fgf10 loss did not appear to affect process of motor neuron segregation into distinct motor columns according to their subtype, however, MMC neurons seemed to be more dispersed in *Fgf10* knockouts.

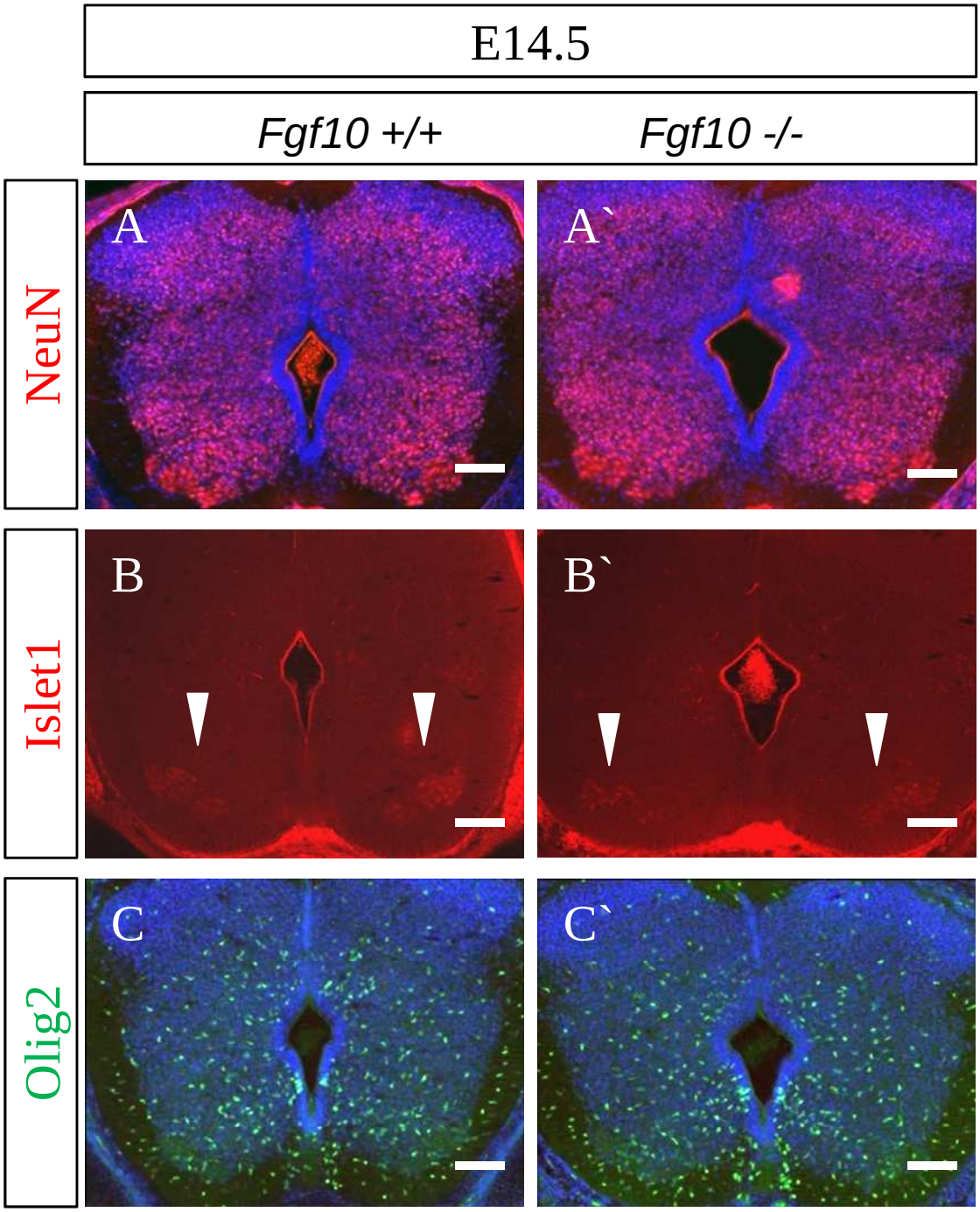

Fig. 3.14. Transverse sections of the spinal cord of wild type and Fgf10 knockout embryos at E14.5. Sections were immunostained with various neuronal and glial markers: ms-NeuN, a marker postmitotic neurons (A and A`) ; ms-Islet1, that marks marks all motor neurons, except LMCl neurons (B and B`); rb-Olig2, a marker of motor neuron and oligodendrocyte progenitors (C and C`); All sections were counterstained with Hoechst, staining specific for cell nuclei. Loss of Fgf10 expression does not appear to affect expression pattern of postmitotic neurons, Islet1+ MN and oligodendrocytes. Scale bars: (A-C`) 100 µm.

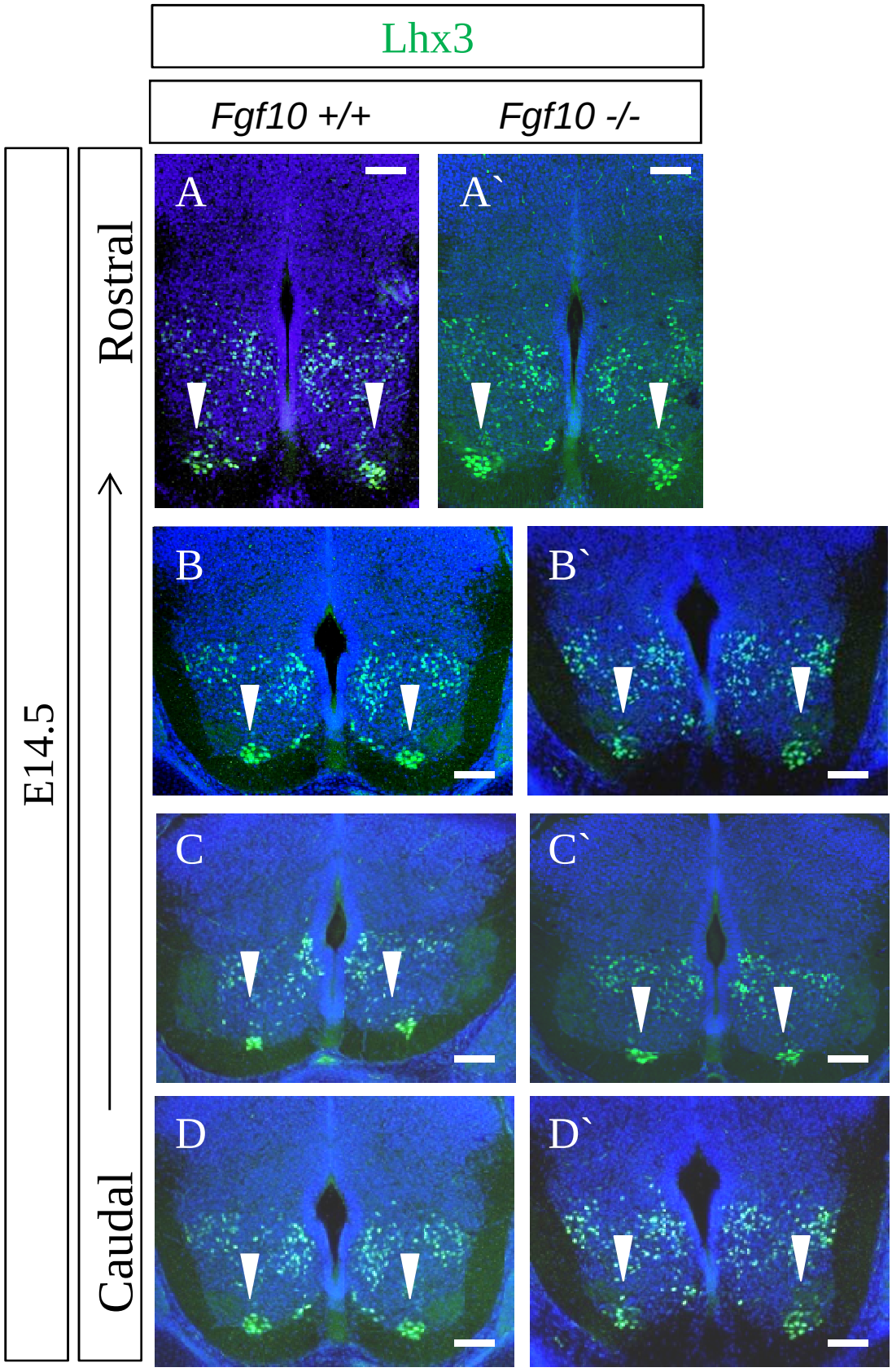

Fig. 3.15. Transverse sections of the spinal cord of wild type and Fgf10 knockout embryos at E14.5 immunostained with rb-Lhx3 and counterstained with Hoechst. Lhx3 is a marker of medial motor column (MMC) neurons and V2 interneurons. Hoechst is a dye, specific for cell nuclei. Absence of Fgf10 expression does not appear to affect number of MMC neurons, however in Fgf10 knockout embryos MMC neurons appear to form more dispersed columns than in wild type. White arrowheads point at MMC. Scale bars: (A-D`) 100 µm.

3.3.4. In *Fgf10* knockout mice axons of motor neurons are misrouted

Previous results showed that the absence of Fgf10 expression did not affect the number of motor neuron and oligodendrocyte progenitors, generation and migration of motor neurons, as well as MN differentiation and segregation into distinct motor columns. The next step was to see if Fgf10 was involved in axonal outgrowth and synapse formation.

Fgf10 knockout and wild type embryos at E10.5 were sectioned in a transverse plane and immunostained with cytoplasmic TuJ1 antibody, which marks neuronal bodies and their processes from the early stage of neuronal differentiation and onwards. Sections of wild type and *Fgf10* knockout embryos were lined up according to the spinal cord and its lumen shape to make sure they were compared at the same level.

It was shown that in *Fgf10* knockouts at brachial level, where normally limbs develop, axons of LMC neurons failed to branch into LMCl and LMCm divisions and formed a cluster of misrouted axons (Fig. 3.16).

These results could suggest that Fgf10 plays role in LMC branching into divisions, although, LMC axons could be misrouted, due to absence of their innervation target, as Fgf10 knockout mice do not have limbs.

At thoracic level, axons of MMC, HMC and PGC neurons were present and project precisely to their targets, dermomyotome, body wall muscles and sympathetic ganglia respectively. However, in the *Fgf10* knockouts MMC axonal terminals appeared to be disordered and in some sections even formed distinct branches (Fig. 3.17).

Obtained results could suggest that Fgf10 plays a role in LMC branching and synapse formation between MMC and dermomyotome, although more *Fgf10* knockout embryos have to be studied (Table 2.1).

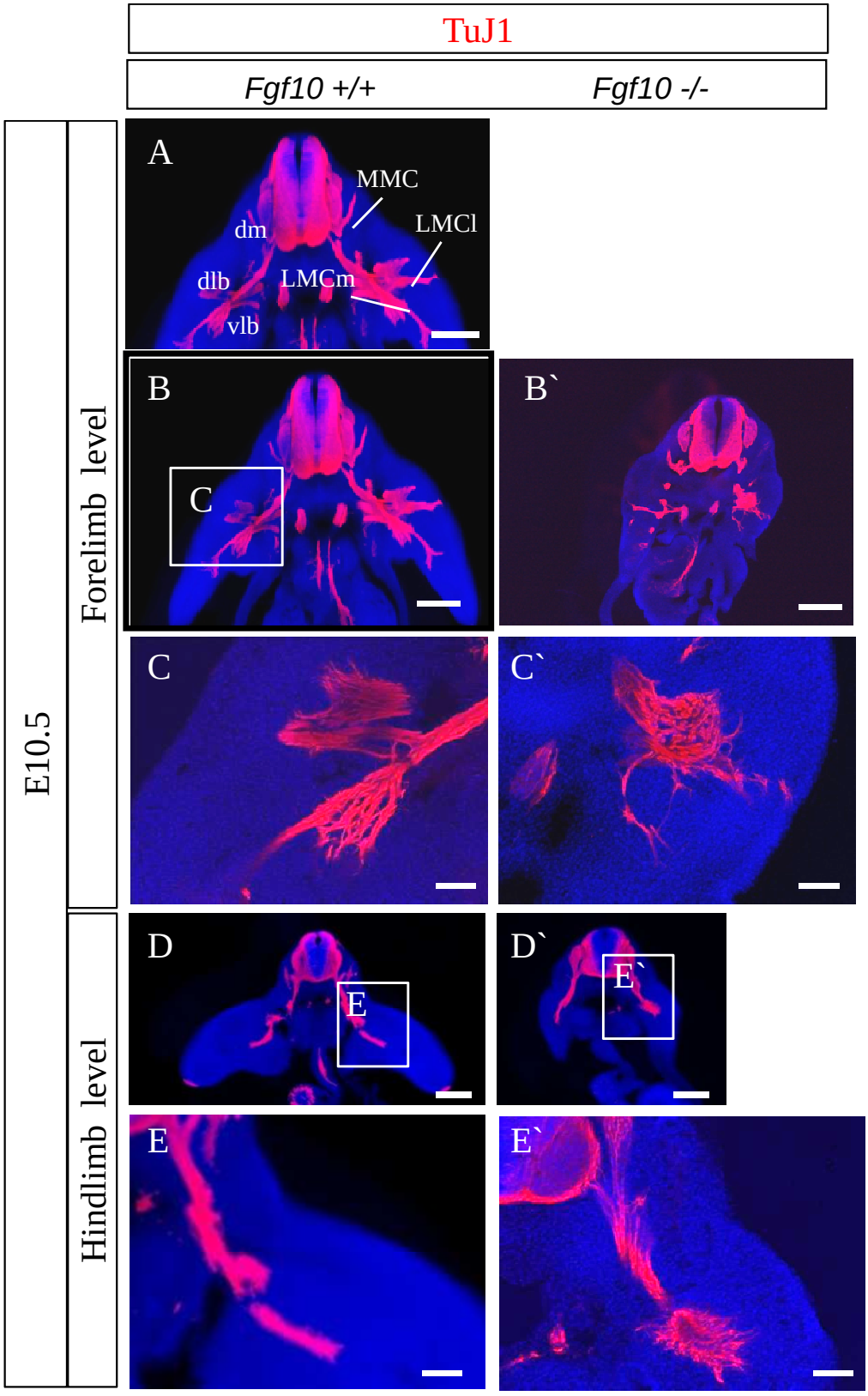

Fig. 3.16. Transverse sections of the spinal cord of wild type and Fgf10 knockout embryos at E10.5 immunostained with ms-TuJ1 and counterstained with Hoechst. TuJ1 (red) marks neurons from the early stage of their differentiation and onwards. Hoechst is cell nuclei specific dye. In Fgf10 knockout embryos, LMC neurons, that normally innervate limbs, fail to branch into LMCm and LMCl divisions. dm- dermomyotome; dlb-dorsal limb bud; vlb –ventral limb bud; MMC-medial motor column; LMCl- Lateral devision of lateral motor column; LMCm – medial devision of lateral motor column. Scale bars: (A-B`, D, D`) 500 µm; (C, C`, E, E`) 100 µm.

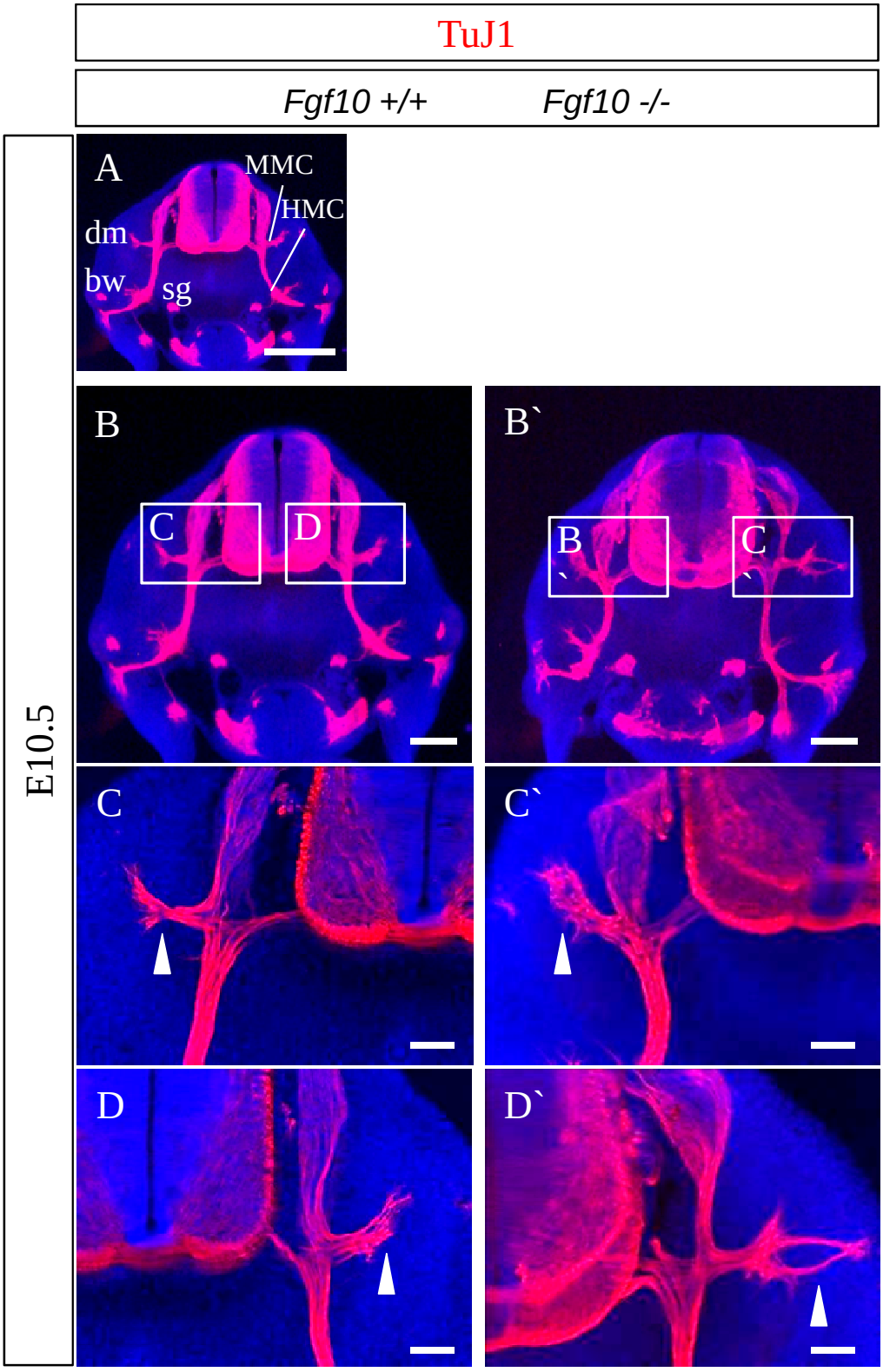

Fig. 3.17. Transverse sections of the spinal cord of wild type and Fgf10 knockout embryos at E10.5 immunostained with ms-TuJ1 and counterstained with Hoechst. TuJ1(red) marks neurons from the early stage of their differentiation and onwards. Hoechst is a dye specific for cell nuclei. In Fgf10 knockout embryos, all subtypes of motor neurons present at thoracic level are able to project axons to their targets, i.e. MMC projects to dermomyotome; HPC to body wall muscles; PGC to sympathetic ganglia; However, in some sections of Fgf10 knockout embryos MMC neurons appear to branch and axonal terminals seem to be disordered. dm-dermomyotome; sg-sympathetic ganglia; bw- body wall muscles; MMC-medial motor column; HMC-hypaxial motor column. Scale bars: (A) 500 µm; (B) 250 µm; (C-D`) 100 µm.

3.4. Development of neurons and progenitors cells appear not to be affected in *FgfR2-IIIc*$^{+/\Delta}$ mice

FgfR2-IIIc$^{+/\Delta}$ mice were used to investigate Fgf10 signalling in the developing mouse spinal cord (Hajihosseini et al., 2001). These transgenic mice lack one copy of *FgfR2-IIIc* that results in a gain-of-function mutation due to a splicing switch within *FgfR2-IIIc* deficient allele. In *FgfR2-IIIc*$^{+/\Delta}$ mice, *Fgfr2-IIIb* isoform is illegitimately expressed along with *Fgfr2-IIIc* at the sites, where normally only *FgfR2-IIIc* is present. That makes the relevant tissues responsive to a broader range of Fgfs than they would normally respond to. *FgfR2-IIIc*$^{+/\Delta}$ mice show Apert syndrome-like phenotype that includes defects in the development of several visceral organs and bones (Hajihosseini et al., 2009).

It was hypothesised that if Fgf10 was expressed in the somas, then some abnormalities in the development of *FgfR2-IIIc*$^{+/\Delta}$ mouse spinal cord were likely to be seen, due to the upregulation of *FgfR2IIIb* isoform in neural tissues, which is otherwise absent (M. K. Hajihosseini personal comments).

Embryos aged E12.5 were isolated, genotyped, and wild type and *FgfR2-IIIc*$^{+/\Delta}$ embryos were then sectioned in a transverse plane. Sections of the spinal cord were immunostained with various neuronal markers, e.g. NeuN, marker for postmitotic neurons; Olig2, marker for motor neuron and oligodendrocyte progenitors; Lhx3, marker for MMC neurons and V2 interneurons.

Patterns of NeuN, Olig2 and Lhx3 expression in the spinal cord were very similar in wild type and *FgfR2-IIIc*$^{+/\Delta}$ embryos (Fig. 3.18). That suggests that the timing of neuronal maturation, generation of MN/OL progenitors and specification of neurons into MMC neurons and V2 neurons was not affected in *FgfR2-IIIc*$^{+/\Delta}$ mice.

Obtained results suggest that in the developing mouse spinal cord, Fgf10 is either transported to neuronal axons or is expressed in the somas and acts in receptor independent manner.

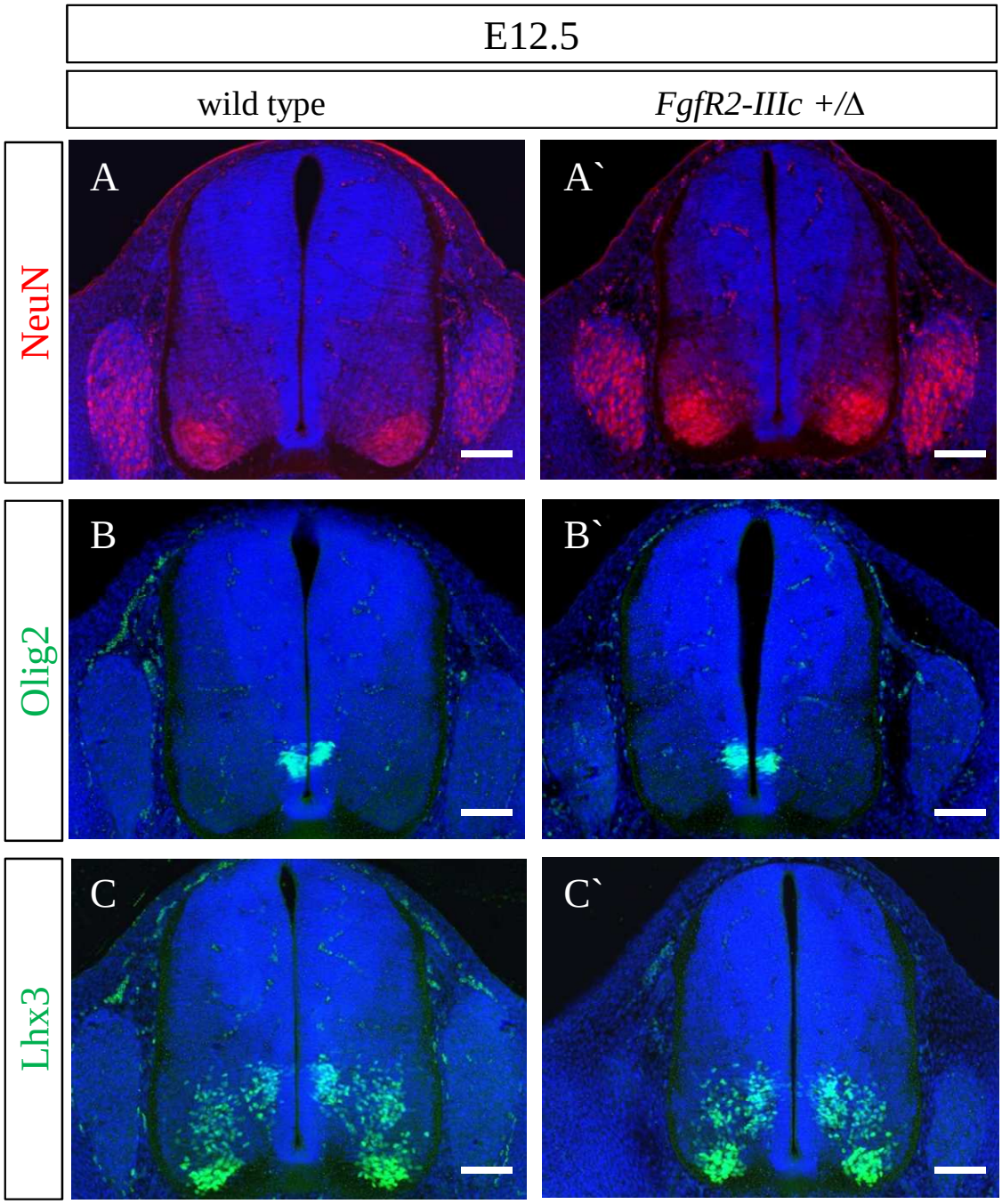

Fig. 3.18. Transverse sections of the spinal cord of wild type and *FgfR2-IIIc* +/Δ mouse embryos at E12.5. Sections were immunostained with ms-NeuN, a marker for postmitotic neurons (A and A`); rb-Olig2, a marker for motor neuron and oligodendrocyte progenitors (B and B`); rb-Lhx3 a marker for MMC motor neurons and V2 interneurons (C and C`). All sections were counterstained with Hoechst, cell nuclei specific dye. No difference in expression pattern of NeuN, Olig2 and Lhx3 could be detected between wild type and *FgfR2-IIIc* +/Δ mouse embryo at E12.5. Scale bars: (A-C`) 100 µm.

4. DISCUSSION

Fgf10 has already been shown to be a multitasking molecule that is of high importance for the normal development of the mouse organism. It plays key roles in limb and lung development, as well as it is very important for the normal development of heart, pancreas, intestine and brain (Bhushan et al., 2001; Kelly et al., 2001; Min et al., 1998; Nyeng et al., 2011; Sahara and O'Leary, 2009). Fgf10 expression has, also, been detected in the spinal cord of 4 and 56 days old mice (Allen Institute for Brain Science database). However, at present, nothing is known about its role in the development of the spinal cord. Fgf10 expression has been detected recently by *in situ* hybridization in the spinal cord of E12.5 mouse embryo, suggesting it does play a role in development. Based on that knowledge, a research project was set up to investigate timing and pattern of Fgf10 expression and its potential role in the development of mouse spinal cord.

4.1. β-gal as a reporter of Fgf10 expression in Fgf10-LacZ mice

Currently, commercial anti-Fgf10 antibodies do not provide any staining. Hence, to examine Fgf10 expression pattern in the developing mouse spinal cord *Fgf10-LacZ* reporter mice have been used. This transgenic mouse line carries a nuclear targeted *LacZ* transgene insertion downstream of *Fgf10* promoter. Hence, the product of the transgene, enzyme β-gal, functions as a reporter of *Fgf10* expression and is present in cells expressing Fgf10 and their descendants (Hajihosseini et al., 2008; Kelly et al., 2001). β-gal is expressed in the cell nucleus and can be detected either enzymatically by a substrate X-gal, which is converted into a blue precipitate by β-gal, or by immunostaining with an anti-β-gal antibody. Rb-anti-β-gal antibody (Millipore) has been shown to provide specific staining in the developing mouse spinal cord and can be used to detect β-gal by immunohistochemitry (Hajihosseini et al., 2008 and our unpublished data).

It is necessary to remember that β-gal expression in *Fgf10-LacZ* mice is nuclear, while Fgf10 molecule could be localized anywhere in the cell, including axons and its terminals, where from it might be secreted later.

In the developing mouse spinal cord, β-gal expressing cells were detected from E8.5 to E15.5, although, it is not known how stable β-gal is and there is a possibility that product of *LacZ* gene may be detected after Fgf10 stops being expressed. Therefore, β-gal expression may not accurately reflect the timing of Fgf10 mRNA expression.

It is possible to tackle this problem either by doing a series of *in situ* hybridizations for Fgf10 at various stages of embryonic development, or by using tamoxifen inducible *Fgf10^{CreERT2} :: ROSA26 LacZ* mouse line (S. Bellusci and M.K. Hajihosseini personal communication). In this transgenic mouse line cytoplasmic expression of *LacZ* gene is induced in Fgf10 expressing cells by tamoxifen. In contrast to *Fgf10-LacZ* mice, in *Fgf10^{CreERT2} :: ROSA26 LacZ* mice, *LacZ* expression is not discontinued when Fgf10 stops being expressed. That allows to induce *LacZ* expression in *Fgf10^{CreERT2} :: ROSA26 LacZ* mice at certain stages of pregnancy, then sacrifice mice and X-gal embryos in order to see if *LacZ* was expressed at the relevant developmental stage.

β-gal can be detected not only in cells that express or used to express Fgf10, but also, in their descendants. However, in the developing spinal cord, β-gal was detected in neurons, but not in their progenitor cells. According to the literature, neurons do not divide anymore after they migrate out of the ventricular zone (Wolpert et al., 2007). Therefore, it seems very unlikely to detect β-gal expression in descendants of Fgf10 expressing cells in the spinal cord.

4.2. Pattern of Fgf10 expression in the developing mouse spinal cord

A clear expression of Fgf10 has been observed in the ventral horns of the developing mouse spinal cord from E9.5 up to E14.5 (Watson et al., 2008). From at least E14.5, Fgf10 expression disappears completely from caudal region of the spinal cord, while it is maintained rostrally, and new areas of its expression appear symmetrically on either side in the dorsal region of the spinal cord. Conversely, studies have shown the presence of Fgf10 expression in the spinal cord of juvenile and adult mice, 4 days and 56 days old, respectively (Allen Institute for Brain Science database). In the spinal cord of a juvenile mouse Fgf10 expressing cells are concentrated in the ventral horns of the spinal cord in the caudal region, while in the spinal cord of an adult mouse Fgf10 is expressed along the entire spinal cord and Fgf10 positive cells are scattered around the grey matter. These observations indicate that Fgf10 might be expressed in a mixed cell population and play diverse roles at different stages of development.

Fgf10 may be expressed in at least two different cell populations. One of them originates at about E14.5 in the dorsal region, rostrally in the spinal cord. As Fgf10 expressing cells are located close to ventricular zone it suggests they recently migrated out and are differentiating. It is known that 80% of oligodendrocyte precursors (OLP) are generated at E12.5-13 from the MN/OL progenitor domain, located in the ventral region of the spinal cord. However, the remaining OLP are produced later at E14.5, from the progenitor domain located in the dorsal region (Cai et al., 2005; Li et al., 2011). Also, it has been shown previously, that certain Fgfs, e.g. Fgf2, are required for oligodendrocyte generation from the dorsal domain of progenitors *in vitro* (Chandran et al., 2003). These facts suggest that Fgf10 expressing cells in

the dorsal domain could possibly be newborn oligodendrocytes. Double labelling at this stage would help to confirm this relationship.

This report focused on the other Fgf10 expressing cell population that originates from the ventral region at E8.5 and later settles in the ventral horns of the spinal cord. It has been noticed that Fgf10 expression in the ventral horns correlated with neurogenesis pattern in the spinal cord, and with the time and pattern of motor neuron generation in particular. MN are first neurons to be born and they are generated in the ventral region of the spinal cord from E9.5 to E13.5, then migrate laterally and settle in the ventral horns of the spinal cord (Watson et al., 2008). Fgf10 expression in the spinal cord resembled this pattern very much. In addition, first neurons are born rostrally and there were more Fgf10 expressing cells in rostral region, which is more mature region of the spinal cord, than caudal (Altman and Bayer, 1984).

Indeed, β-gal has been detected in early differentiated neurons and in motor neurons in the developing spinal cord of *Fgf10-LacZ* mice. It is not known, whether β-gal positive mature neurons still express Fgf10, but it is nice to speculate that Fgf10 could be expressed in postmitotic cells. Previously, Fgf10 was mainly reported to be involved in cell proliferation and progenitor domain maintenance, e.g. in white adipose tissue and intestine (Konishi et al., 2006; Nyeng et al., 2011; Nyeng et al., 2007).

4.3. Potential roles of Fgf10 in the development of mouse spinal cord

In the developing mouse spinal cord Fgf10 expression has been detected in early differentiated neurons and later in motor neurons. The timing of Fgf10 expression in the ventral region of the spinal cord correlates with motor neuron birth and maturation. These observations suggested Fgf10 has a role in the development of the ventral region of the spinal cord and in MN generation and differentiation in particular. Fgf10 could be involved in transition from progenitor cells to mature neurons; MN differentiation into particular subtypes; segregation into motor columns; axonal outgrowth and/or navigation to subtype specifc targets; synaptogenesis or cell death.

4.3.1. Potential role of Fgf10 in MN identity and their transition from progenitor cells to motor neurons during neurogenesis in the developing mouse spinal cord

Initially, Fgf10 expression in the spinal cord is detected in early differentiated neurons, which lie in motor neuron and oligodendrocyte progenitor domain. That suggests Fgf10 expression enables motor neuron progenitors to exit their cell cycle and become early born

motor neurons, in such a way regulating identity of motor neurons, as well as timing of their generation and their quantity.

Obtained results show that Fgf10 expression is not necessary for motor neurons to become postmitotic and it does not seem to play role in MN identity. In the absence of Fgf10 expression neurons were able to exit their cell cycle and MMC neurons were generated at the same time and quantity as in wild type.

Also, it was hypothesised that if Fgf10 was involved in motor neuron identity, in the spinal cord of Fgf10 knockouts fate switch might take place, i.e. progenitors that were meant to become motor neurons, might differentiate into oligodendrocytes that are generated from the same progenitors domain. Results show that Fgf10 is unlikely to play role in motor neuron identity, because in Fgf10 knockouts at E10.5 and E14.5 amount of MMC neurons and OL progenitors and precursors was the same as in wild type.

However, not all MN subtypes were visualised and compared during this study and there is a possibility that there might be a fate switch in motor neuronal subtypes. To exclude or confirm Fgf10 role in motor neuron identity, further research should be performed with all MN subtypes included into the study.

4.3.2. Potential role of Fgf10 in MN differentiation into particular subtypes and segregation into motor columns

Fgf10 expression has been detected in differentiating and mature motor neurons that suggested its role in motor neuron differentiation and migration to their final positions according to their neuronal subtype. Achieved results show that in the absence of Fgf10 expression motor neurons are able to migrate and to segregate into distinct motor columns.

Fgf10 expression has not been assigned to any particular MN subtype, but at E12 it was mainly detected in MMC neuron domain, which suggests its role in the development of this particular type of MN. However, Fgf10 absence did not affect MMC subtype generation and migration to the final position medially in the ventral horns.

Interestingly, at E14.5 MMC neurons in Fgf10 knockouts seemed to be more dispersed than in wild type. That suggests Fgf10 role either in timing of MMC neuron migration to their final position or organization of MMC neurons into a discrete column.

4.3.3. Potential role of Fgf10 in axonal outgrowth and guidance of motor neurons to innervation targets according to their subtype

β-gal faithfully reports Fgf10 expression in a particular cell, however, the site of Fgf10 localization in the cell can not be detected through β-gal expression. Fgf10 molecule could be located and secreted from any part of the motor neuron, including axons. That suggests Fgf10 role as a guidance molecule and its involvement in the outgrowth of motor axons and their projection to specific muscles. Fgfs have been shown previously to play role of chemoattractants, e.g. Fgf8 has been shown to attract MMC neurons to the dermomyotome (Shirasaki et al., 2006); Fgf10 has been shown to act as a chemoattractant for the lung epithelium during development (Park et al., 1998). Fgf10 could play a role of the guiding molecule for motor neuron axons.

Axonal projections of all motor neuron subtypes, except LMC neurons, were able to develop, exit ventrally of the spinal cord and project to their target muscles according to their subtypes. At the limb level, LMC neurons that innervate limb muscles failed to branch into LMCl and LMCm divisions and formed a cluster of disordered axonal terminals. Possible explanation could be that Fgf10 knockout embryos do not have limbs and LMC neurons lack their innervation target in this mutant.

These results suggest that Fgf10 is unlikely to have a role in axonal outgrowth and guidance to their innervation targets. Further studies using limbless Fgf10 expressing mutant mouse as a positive control would be necessary.

4.3.4. Potential role of Fgf10 in synapse formation between terminals of MN axons and their target muscles

In the spinal cord of Fgf10 knockout embryos LMC neurons fail to branch and instead form a disordered cluster of axonal terminals. In addition, axonal terminals of MMC neurons appear to look disordered and in some sections even branch out. Fgf 22 and its closest relatives (Fgf7 and Fgf10) have, already, been implied a role in synapse formation in the mammalian brain and it is very likely that Fgf10 may be involved in synaptogenesis in the spinal cord (Umemori et al., 2004).

In addition, Fgf10 expression has been detected in the ventral horns of the spinal cord in a juvenile mouse, aged 4 days. Knowing that maturation of a neuromuscular junction takes up to 3 weeks in rodents, it can be suggested that Fgf10 is involved in synapse maturation postnatally as well (Wolpert et al., 2007)

Further research on Fgf10 role in synaptogenesis has to be performed *in vivo* and *in vitro*. For example, coculture primary motor neurons, from embryonic mouse spinal cord, and myoblasts, to investigate Fgf10 role in synapse formation *in vitro*.

4.3.5. Potential role of Fgf10 in motor neuron survival during cell death

Neuronal death is a natural event occurring about the time when motor neuronal axons are reaching their target muscles, and that continues even after synapses have been established, until each muscle fiber is innervated by axon terminals from one motor neuron (Wolpert et al., 2007). As Fgf10 is expressed in a subset of motor neurons during their differentiation that includes cell death, it could be involved either in promoting neuronal cell death or play role in MN survival.

It has been shown in chicken, that the number of surviving motor neurons depends on the amount of limb musculature, in the absence of the limb bud the amount of motor neurons decreased severely (Lanser and Fallon, 1987). As Fgf10 knockout embryos are limbless and, therefore, lack targets for axonal projections, it was hypothesised that in Fgf10 knockout embryos there should be less motor neurons present due to enhanced cell death, even if Fgf10 is not involved in MN survival. Surprisingly, in limbless mouse embryos the amount of motor axons did not seem to be reduced.

These results could suggest Fgf10 role in promoting cell death, however further studies are necessary. Employing another limbless mutant, for example Lef1(-/-)Tcf1(-/-) as a positive control, would be an advantage (Galceran et al., 1999).

4.4. Fgf10 signalling in the developing mouse spinal cord

β-gal is a faithful reporter of Fgf10 expression in *Fgf10-LacZ* mice. However, it does not provide information in which part of the cell Fgf10 is expressed. It could be expressed either in the cell bodies located in the grey matter of the spinal cord or in the neuronal axons. FgfR2-IIIc isoform has been shown to be predominant in the adult CNS, including the spinal cord (Fon Tacer et al., 2010). In the developing mouse spinal cord FgfR2 isoform has not been identified, but it is known that in the other parts of developing CNS, FgfR2-IIIc isoform is abundant (personal communication with M. K. Hajihosseini). Therefore, it has been assumed that in the developing mouse spinal cord FgfR2-IIIc isoform is present. If Fgf10, which normally signals through FgfR2-IIIb isoform, was expressed in the cell bodies, most probably it would have signalled independently of the receptor.

To investigate Fgf10 signaling in the developing mouse spinal cord, *FgfR2-IIIc*$^{+/\Delta}$ mice were used. These mice, due to a gain-of-function mutation, express both FgfR2 isoforms in neural and mesenchymal tissues, where normally only FgfR2-IIIc would be expressed.

It was predicted that if Fgf10 molecule was secreted in the spinal cord, then there would be some differences in neuronal and/or MN/OL progenitor expression pattern in *FgfR2-IIIc*$^{+/\Delta}$ mice compared to wild type, because it would activate FgfR2-IIIb isoform that normally is not present.

FgfR2-IIIc$^{+/\Delta}$ mice showed no abnormalities in the spinal cord. This indicates that Fgf10 is either expressed in motor neuron bodies and functions in receptor-independent manner, or transported to the motor neuronal axons or their terminals.

Further work has to be performed to characterize the way Fgf10 mediates its signalling in the spinal cord. For example, to identify FgfR2 receptor isoform in the developing mouse spinal cord through RT-PCR or immunohistochemistry in the wild type and in *FgfR2-IIIc*$^{+/\Delta}$ mice.

4.5. Future directions

Fgf10`s role still has to be elucidated and it is of high importance to continue research about Fgf10 involvement in the development of mouse spinal cord and motor neurons in particular. It has already been shown that Fgf10 is expressed during motor neuron differentiation and maturation, and may have a key role at one of the stages, for example in synapse formation. If its role during normal development will be determined, it potentially can further our understanding of the mechanisms of neurodegenerative diseases, such as ALS, and promote clinical therapies for patients with spinal cord injuries or suffering from motor neuron diseases. In addition, knowing Fgf10 role in normal MN development could provide novel insight into stem cell differentiation *in vitro* into distinct neuronal subtypes.

REFERENCES

Allen Institute for Brain Science database (2011). Mouse Spinal Cord. Fgf10. Available at http://mousespinal.brain-map.org/imageseries/list/1.html?gene_term=fgf10&searchSym=t&searchAlt=t&searchName=t&excludeFail=on&commit=Search Last accessed 27th October 2011.

Abler, L. L., Mansour, S. L. and Sun, X. (2009). Conditional gene inactivation reveals roles for Fgf10 and Fgfr2 in establishing a normal pattern of epithelial branching in the mouse lung. *Dev Dyn* **238**, 1999-2013.

Altman, J. and Bayer, S. A. (1984). The development of the rat spinal cord. *Adv Anat Embryol Cell Biol* **85**, 1-164.

Bellusci, S., Grindley, J., Emoto, H., Itoh, N. and Hogan, B. L. (1997). Fibroblast growth factor 10 (FGF10) and branching morphogenesis in the embryonic mouse lung. *Development* **124**, 4867-78.

Berg, T., Rountree, C. B., Lee, L., Estrada, J., Sala, F. G., Choe, A., Veltmaat, J. M., De Langhe, S., Lee, R., Tsukamoto, H. et al. (2007). Fibroblast growth factor 10 is critical for liver growth during embryogenesis and controls hepatoblast survival via beta-catenin activation. *Hepatology* **46**, 1187-97.

Bhushan, A., Itoh, N., Kato, S., Thiery, J. P., Czernichow, P., Bellusci, S. and Scharfmann, R. (2001). Fgf10 is essential for maintaining the proliferative capacity of epithelial progenitor cells during early pancreatic organogenesis. *Development* **128**, 5109-17.

Bonanomi, D. and Pfaff, S. L. (2010). Motor axon pathfinding. *Cold Spring Harb Perspect Biol* **2**, a001735.

Briscoe, J. and Novitch, B. G. (2008). Regulatory pathways linking progenitor patterning, cell fates and neurogenesis in the ventral neural tube. *Philos Trans R Soc Lond B Biol Sci* **363**, 57-70.

Briscoe, J., Pierani, A., Jessell, T. M. and Ericson, J. (2000). A homeodomain protein code specifies progenitor cell identity and neuronal fate in the ventral neural tube. *Cell* **101**, 435-45.

Bronner-Fraser, M. and Fraser, S. E. (1997). Differentiation of the vertebrate neural tube. *Curr Opin Cell Biol* **9**, 885-91.

Cai, J., Qi, Y., Hu, X., Tan, M., Liu, Z., Zhang, J., Li, Q., Sander, M. and Qiu, M. (2005). Generation of oligodendrocyte precursor cells from mouse dorsal spinal cord independent of Nkx6 regulation and Shh signaling. *Neuron* **45**, 41-53.

Carlesi, C., Pasquali, L., Piazza, S., Lo Gerfo, A., Caldarazzo Ienco, E., Alessi, R., Fornai, F. and Siciliano, G. (2011). Strategies for clinical approach to neurodegeneration in Amyotrophic lateral sclerosis. *Arch Ital Biol* **149**, 151-67.

Chan, W. Y., Kohsaka, S. and Rezaie, P. (2007). The origin and cell lineage of microglia: new concepts. *Brain Res Rev* **53**, 344-54.

Chandran, S., Kato, H., Gerreli, D., Compston, A., Svendsen, C. N. and Allen, N. D. (2003). FGF-dependent generation of oligodendrocytes by a hedgehog-independent pathway. *Development* **130**, 6599-609.

Colon-Ramos, D. A. (2009). Synapse formation in developing neural circuits. *Curr Top Dev Biol* **87**, 53-79.

Colvin, J. S., Feldman, B., Nadeau, J. H., Goldfarb, M. and Ornitz, D. M. (1999). Genomic organization and embryonic expression of the mouse fibroblast growth factor 9 gene. *Dev Dyn* **216**, 72-88.

Corcia, P., Praline, J., Vourc'h, P. and Andres, C. (2008). Genetics of motor neuron disorders. *Rev Neurol (Paris)* **164**, 115-30.

Crossley, P. H. and Martin, G. R. (1995). The mouse Fgf8 gene encodes a family of polypeptides and is expressed in regions that direct outgrowth and patterning in the developing embryo. *Development* **121**, 439-51.

Dasen, J. S. and Jessell, T. M. (2009). Hox networks and the origins of motor neuron diversity. *Curr Top Dev Biol* **88**, 169-200.

Dasen, J. S., Liu, J. P. and Jessell, T. M. (2003). Motor neuron columnar fate imposed by sequential phases of Hox-c activity. *Nature* **425**, 926-33.

Dasen, J. S., Tice, B. C., Brenner-Morton, S. and Jessell, T. M. (2005). A Hox regulatory network establishes motor neuron pool identity and target-muscle connectivity. *Cell* **123**, 477-91.

Dessaud, E., McMahon, A. P. and Briscoe, J. (2008). Pattern formation in the vertebrate neural tube: a sonic hedgehog morphogen-regulated transcriptional network. *Development* **135**, 2489-503.

Doretto, S., Malerba, M., Ramos, M., Ikrar, T., Kinoshita, C., De Mei, C., Tirotta, E., Xu, X. and Borrelli, E. (2011). Oligodendrocytes as regulators of neuronal networks during early postnatal development. *PLoS One* **6**, e19849.

Eisen, J. S. (1999). Patterning motoneurons in the vertebrate nervous system. *Trends Neurosci* **22**, 321-6.

Ericson, J., Morton, S., Kawakami, A., Roelink, H. and Jessell, T. M. (1996). Two critical periods of Sonic Hedgehog signaling required for the specification of motor neuron identity. *Cell* **87**, 661-73.

Eswarakumar, V. P., Lax, I. and Schlessinger, J. (2005). Cellular signaling by fibroblast growth factor receptors. *Cytokine Growth Factor Rev* **16**, 139-49.

Fon Tacer, K., Bookout, A. L., Ding, X., Kurosu, H., John, G. B., Wang, L., Goetz, R., Mohammadi, M., Kuro-o, M., Mangelsdorf, D. J. et al. (2010). Research resource:

Comprehensive expression atlas of the fibroblast growth factor system in adult mouse. *Mol Endocrinol* **24**, 2050-64.

Ford-Perriss, M., Abud, H. and Murphy, M. (2001). Fibroblast growth factors in the developing central nervous system. *Clin Exp Pharmacol Physiol* **28**, 493-503.

Galceran, J., Farinas, I., Depew, M. J., Clevers, H. and Grosschedl, R. (1999). Wnt3a-/--like phenotype and limb deficiency in Lef1(-/-)Tcf1(-/-) mice. *Genes Dev* **13**, 709-17.

Garces, A., Nishimune, H., Philippe, J. M., Pettmann, B. and deLapeyriere, O. (2000). FGF9: a motoneuron survival factor expressed by medial thoracic and sacral motoneurons. *J Neurosci Res* **60**, 1-9.

Hajihosseini, M. K., De Langhe, S., Lana-Elola, E., Morrison, H., Sparshott, N., Kelly, R., Sharpe, J., Rice, D. and Bellusci, S. (2008). Localization and fate of Fgf10-expressing cells in the adult mouse brain implicate Fgf10 in control of neurogenesis. *Mol Cell Neurosci* **37**, 857-68.

Hajihosseini, M. K., Duarte, R., Pegrum, J., Donjacour, A., Lana-Elola, E., Rice, D. P., Sharpe, J. and Dickson, C. (2009). Evidence that Fgf10 contributes to the skeletal and visceral defects of an Apert syndrome mouse model. *Dev Dyn* **238**, 376-85.

Hajihosseini, M. K., Wilson, S., De Moerlooze, L. and Dickson, C. (2001). A splicing switch and gain-of-function mutation in FgfR2-IIIc hemizygotes causes Apert/Pfeiffer-syndrome-like phenotypes. *Proc Natl Acad Sci U S A* **98**, 3855-60.

Itoh, N. and Ornitz, D. M. (2008). Functional evolutionary history of the mouse Fgf gene family. *Dev Dyn* **237**, 18-27.

Jaye, M., Schlessinger, J. and Dionne, C. A. (1992). Fibroblast growth factor receptor tyrosine kinases: molecular analysis and signal transduction. *Biochim Biophys Acta* **1135**, 185-99.

Jessell, T. M. (2000). Neuronal specification in the spinal cord: inductive signals and transcriptional codes. *Nat Rev Genet* **1**, 20-9.

Kania, A. and Jessell, T. M. (2003). Topographic motor projections in the limb imposed by LIM homeodomain protein regulation of ephrin-A:EphA interactions. *Neuron* **38**, 581-96.

Kania, A., Johnson, R. L. and Jessell, T. M. (2000). Coordinate roles for LIM homeobox genes in directing the dorsoventral trajectory of motor axons in the vertebrate limb. *Cell* **102**, 161-73.

Kanning, K. C., Kaplan, A. and Henderson, C. E. (2010). Motor Neuron Diversity in Development and Disease. *Annual Review of Neuroscience, Vol 33* **33**, 409-440.

Kelly, R. G., Brown, N. A. and Buckingham, M. E. (2001). The arterial pole of the mouse heart forms from Fgf10-expressing cells in pharyngeal mesoderm. *Dev Cell* **1**, 435-40.

Kettenmann, H., Hanisch, U. K., Noda, M. and Verkhratsky, A. (2011). Physiology of microglia. *Physiol Rev* **91**, 461-553.

Kmita, M. and Duboule, D. (2003). Organizing axes in time and space; 25 years of colinear tinkering. *Science* **301**, 331-3.

Komi-Kuramochi, A., Kawano, M., Oda, Y., Asada, M., Suzuki, M., Oki, J. and Imamura, T. (2005). Expression of fibroblast growth factors and their receptors during full-thickness skin wound healing in young and aged mice. *J Endocrinol* **186**, 273-89.

Konishi, M., Asaki, T., Koike, N., Miwa, H., Miyake, A. and Itoh, N. (2006). Role of Fgf10 in cell proliferation in white adipose tissue. *Mol Cell Endocrinol* **249**, 71-7.

Kouhara, H., Hadari, Y. R., Spivak-Kroizman, T., Schilling, J., Bar-Sagi, D., Lax, I. and Schlessinger, J. (1997). A lipid-anchored Grb2-binding protein that links FGF-receptor activation to the Ras/MAPK signaling pathway. *Cell* **89**, 693-702.

Lanser, M. E. and Fallon, J. F. (1987). Development of the brachial lateral motor column in the wingless mutant chick embryo: motoneuron survival under varying degrees of peripheral load. *J Comp Neurol* **261**, 423-34.

Leclerc, C., Neant, I. and Moreau, M. (2011). Early neural development in vertebrates is also a matter of calcium. *Biochimie*.

Lee, A. and Pow, D. V. (2010). Astrocytes: Glutamate transport and alternate splicing of transporters. *Int J Biochem Cell Biol* **42**, 1901-6.

Li, H., de Faria, J. P., Andrew, P., Nitarska, J. and Richardson, W. D. (2011). Phosphorylation regulates OLIG2 cofactor choice and the motor neuron-oligodendrocyte fate switch. *Neuron* **69**, 918-29.

Luria, V., Krawchuk, D., Jessell, T. M., Laufer, E. and Kania, A. (2008). Specification of motor axon trajectory by ephrin-B:EphB signaling: symmetrical control of axonal patterning in the developing limb. *Neuron* **60**, 1039-53.

Mailleux, A. A., Spencer-Dene, B., Dillon, C., Ndiaye, D., Savona-Baron, C., Itoh, N., Kato, S., Dickson, C., Thiery, J. P. and Bellusci, S. (2002). Role of FGF10/FGFR2b signaling during mammary gland development in the mouse embryo. *Development* **129**, 53-60.

Maruoka, Y., Ohbayashi, N., Hoshikawa, M., Itoh, N., Hogan, B. L. and Furuta, Y. (1998). Comparison of the expression of three highly related genes, Fgf8, Fgf17 and Fgf18, in the mouse embryo. *Mech Dev* **74**, 175-7.

McWhirter, J. R., Goulding, M., Weiner, J. A., Chun, J. and Murre, C. (1997). A novel fibroblast growth factor gene expressed in the developing nervous system is a downstream target of the chimeric homeodomain oncoprotein E2A-Pbx1. *Development* **124**, 3221-32.

Min, H., Danilenko, D. M., Scully, S. A., Bolon, B., Ring, B. D., Tarpley, J. E., DeRose, M. and Simonet, W. S. (1998). Fgf-10 is required for both limb and lung development and exhibits striking functional similarity to Drosophila branchless. *Genes Dev* **12**, 3156-61.

Muroyama, Y., Fujihara, M., Ikeya, M., Kondoh, H. and Takada, S. (2002). Wnt signaling plays an essential role in neuronal specification of the dorsal spinal cord. *Genes Dev* **16**, 548-53.

Murphy, M., Reid, K., Ford, M., Furness, J. B. and Bartlett, P. F. (1994). FGF2 regulates proliferation of neural crest cells, with subsequent neuronal differentiation regulated by LIF or related factors. *Development* **120**, 3519-28.

Nave, K. A. (2010). Myelination and support of axonal integrity by glia. *Nature* **468**, 244-52.

Nornes, H. O. and Carry, M. (1978). Neurogenesis in spinal cord of mouse: an autoradiographic analysis. *Brain Res* **159**, 1-6.

Novitch, B. G., Wichterle, H., Jessell, T. M. and Sockanathan, S. (2003). A requirement for retinoic acid-mediated transcriptional activation in ventral neural patterning and motor neuron specification. *Neuron* **40**, 81-95.

Nyeng, P., Bjerke, M. A., Norgaard, G. A., Qu, X., Kobberup, S. and Jensen, J. (2011). Fibroblast growth factor 10 represses premature cell differentiation during establishment of the intestinal progenitor niche. *Dev Biol* **349**, 20-34.

Nyeng, P., Norgaard, G. A., Kobberup, S. and Jensen, J. (2007). FGF10 signaling controls stomach morphogenesis. *Dev Biol* **303**, 295-310.

Ohbayashi, N., Shibayama, M., Kurotaki, Y., Imanishi, M., Fujimori, T., Itoh, N. and Takada, S. (2002). FGF18 is required for normal cell proliferation and differentiation during osteogenesis and chondrogenesis. *Genes Dev* **16**, 870-9.

Ornitz, D. M. and Itoh, N. (2001). Fibroblast growth factors. *Genome Biol* **2**, REVIEWS3005.

Park, H. C. and Appel, B. (2003). Delta-Notch signaling regulates oligodendrocyte specification. *Development* **130**, 3747-55.

Park, W. Y., Miranda, B., Lebeche, D., Hashimoto, G. and Cardoso, W. V. (1998). FGF-10 is a chemotactic factor for distal epithelial buds during lung development. *Dev Biol* **201**, 125-34.

Price, S. R. and Briscoe, J. (2004). The generation and diversification of spinal motor neurons: signals and responses. *Mech Dev* **121**, 1103-15.

Rowland, L. P. (2010). Progressive muscular atrophy and other lower motor neuron syndromes of adults. *Muscle Nerve* **41**, 161-5.

Sahara, S. and O'Leary, D. D. (2009). Fgf10 regulates transition period of cortical stem cell differentiation to radial glia controlling generation of neurons and basal progenitors. *Neuron* **63**, 48-62.

Sanes, D. H., Reh, T. A., Harris, W. A. (2006). Development of the nervous system. Second edition. *Academic press*, 373 pages.

Sharma, K., Sheng, H. Z., Lettieri, K., Li, H., Karavanov, A., Potter, S., Westphal, H. and Pfaff, S. L. (1998). LIM homeodomain factors Lhx3 and Lhx4 assign subtype identities for motor neurons. *Cell* **95**, 817-28.

Shaw, P. J. (2005). Molecular and cellular pathways of neurodegeneration in motor neurone disease. *J Neurol Neurosurg Psychiatry* **76**, 1046-57.

Shirasaki, R., Lewcock, J. W., Lettieri, K. and Pfaff, S. L. (2006). FGF as a target-derived chemoattractant for developing motor axons genetically programmed by the LIM code. *Neuron* **50**, 841-53.

Slack, J.M.V. (2006). Essential developmental biology. Second edition. *Blackwell Publishing Ltd.*, 365 pages.

Smallwood, P. M., Munoz-Sanjuan, I., Tong, P., Macke, J. P., Hendry, S. H., Gilbert, D. J., Copeland, N. G., Jenkins, N. A. and Nathans, J. (1996). Fibroblast growth factor (FGF) homologous factors: new members of the FGF family implicated in nervous system development. *Proc Natl Acad Sci U S A* **93**, 9850-7.

Tagashira, S., Harada, H., Katsumata, T., Itoh, N. and Nakatsuka, M. (1997). Cloning of mouse FGF10 and up-regulation of its gene expression during wound healing. *Gene* **197**, 399-404.

Tao, H., Shimizu, M., Kusumoto, R., Ono, K., Noji, S. and Ohuchi, H. (2005). A dual role of FGF10 in proliferation and coordinated migration of epithelial leading edge cells during mouse eyelid development. *Development* **132**, 3217-30.

Traub, R., Mitsumoto, H. and Rowland, L. P. (2011). Research advances in amyotrophic lateral sclerosis, 2009 to 2010. *Curr Neurol Neurosci Rep* **11**, 67-77.

Tsuchida, T., Ensini, M., Morton, S. B., Baldassare, M., Edlund, T., Jessell, T. M. and Pfaff, S. L. (1994). Topographic organization of embryonic motor neurons defined by expression of LIM homeobox genes. *Cell* **79**, 957-70.

Ulloa, F. and Marti, E. (2010). Wnt won the war: antagonistic role of Wnt over Shh controls dorso-ventral patterning of the vertebrate neural tube. *Dev Dyn* **239**, 69-76.

Umemori, H., Linhoff, M. W., Ornitz, D. M. and Sanes, J. R. (2004). FGF22 and its close relatives are presynaptic organizing molecules in the mammalian brain. *Cell* **118**, 257-70.

Vega-Hernandez, M., Kovacs, A., De Langhe, S. and Ornitz, D. M. (2011). FGF10/FGFR2b signaling is essential for cardiac fibroblast development and growth of the myocardium. *Development* **138**, 3331-40.

Watson, C., Paxinos, G., Kayalioglu, G. (2008). The Spinal Cord. *Academic Press*, 387 pages.

Webb, S. E., Lee, K. K., Tang, M. K. and Ede, D. A. (1997). Fibroblast growth factors 2 and 4 stimulate migration of mouse embryonic limb myogenic cells. *Dev Dyn* **209**, 206-16.

Wilson, L. and Maden, M. (2005). The mechanisms of dorsoventral patterning in the vertebrate neural tube. *Dev Biol* **282**, 1-13.

Wolpert, L., Jessell, T., Lawrence, P., Meyerovitz, E., Robertson, E., Smith, J. (2007). Principles of Development. Third edition. *Oxford University Press*, 551 pages.

Yamamoto, Y. and Henderson, C. E. (1999). Patterns of programmed cell death in populations of developing spinal motoneurons in chicken, mouse, and rat. *Dev Biol* **214**, 60-71.

Yamasaki, M., Miyake, A., Tagashira, S. and Itoh, N. (1996). Structure and expression of the rat mRNA encoding a novel member of the fibroblast growth factor family. *J Biol Chem* **271**, 15918-21.

Zakany, J., Zacchetti, G. and Duboule, D. (2007). Interactions between HOXD and Gli3 genes control the limb apical ectodermal ridge via Fgf10. *Dev Biol* **306**, 883-93.